Multi-GeV Plasma Wakefield Acceleration Experiments

The E-167 Collaboration:

F.-J. Decker, P. Emma, M. J. Hogan, R. Ischebeck,*

R. H. Iverson, P. Krejcik, R. H. Siemann and D. Walz

Stanford Linear Accelerator Center

C. E. Clayton, C. Huang, D. K. Johnson, C. Joshi,*

W. Lu, K. A. Marsh, W. B. Mori and M. Zhou

University of California, Los Angeles

S. Deng, B. Feng, T. Katsouleas, P. Muggli and E. Oz*

University of Southern California

2005-01-14

1 Abstract

In the past five years plasma wakefield accelerators have emerged as a leading advanced accelerator scheme due to progress on a number of fronts (see [1]). The SLAC/UCLA/USC E-162/164 collaboration has been arguably the lead group pioneering this research. Accomplishments include the first demonstration that controlled beam propagation and high-gradient acceleration could be extended from the mm scale to meter scales (E-157 and E-162), the first acceleration of positrons (E-162) in a plasma and most recently the first acceleration of electrons by more than one GeV (E-164X). These experiments have yielded a number of rich new beam and plasma physics results, demonstrated the promise of beam-driven plasma accelerators and developed a sophisticated laboratory infrastructure for beam and plasma experiments in the Final Focus Test Beam (FFTB).

This proposal aims to capitalize on that foundation with even more ambitious goals. We propose to extend the plasma wakefield acceleration experiments, pushing the advanced accelerator frontier to possibly as high as 10 GeV. We further propose to explore longitudinal bunch shaping techniques capable of providing the bunch distributions needed for studying acceleration of mono-energetic beams in a future afterburner based on plasma wakefields.

These follow-up experiments are based on the existing apparatus. In extending the plasma length to 30 cm and the energy reach to 10 GeV, the new experiments will enter a regime in which an initial tilt of the incoming beam could be amplified by the electron hose instability, leading to the break-up of the beam by the plasma. This effect could limit the applicability of plasma accelerators, and will therefore be an integral part of the studies.

Furthermore, the possibility of using the high X-ray flux from the beam's betatron/synchrotron radiation in the plasma to produce a novel positron source will be explored in more detail. Exploratory experiments on electrons that are self-trapped from the plasma (plasma dark current) and on fast ions are planned. New and improved diagnostics will allow for a better measurement of the beam current distribution and help understanding the processes in the plasma.

2 Introduction

During the last century, particle accelerators have steadily increased their energy, leading to extraordinary discoveries about the structure of the universe and finding their way into many practical applications from television tubes to medical diagnostics and treatment. The maximum particle energy has increased exponentially, increasing by a factor of 10 every decade.

However, the growth in electron/positron accelerator energy seems to have begun to level off in the last decades (see **Figure 1**). This has been attributed to the fact that the technology of accelerating these particles with radiofrequency cavities is approaching its limits [2].

Various technologies have been proposed to extend the energy reach of these particle accelerators. Some extend existing RF technologies to higher frequencies or use dielectrics. However, they are all limited by breakdown on the material surface. This could be overcome by using a plasma as accelerating medium, where the limit is several orders of magnitude greater.

Investigating the acceleration of particles and beams to very high energy in large gradient plasma modules therefore offer great potentials for future accelerators. In particular, the beam-driven or plasma wakefield accelerator (PWFA) scheme proposed by Fainberg et al. [3] could be used to double the energy of a future linear collider [4].

The basic concept of the plasma wakefield accelerator involves the passage of an ultra-relativistic electron bunch through a stationary plasma [5]. The plasma can be formed by ionizing a gas with a laser (as done in experiments E-157 and E-162), or through field-ionization by the Coulomb field of the relativistic bunch (experiments E-164 and E-164X). The head of the bunch drives a wake in the plasma, while the particles in the back witness the resulting acceleration (see **Figure 2**). The system effectively functions as a transformer, where the energy from the particles in the head is transferred to those in the back.

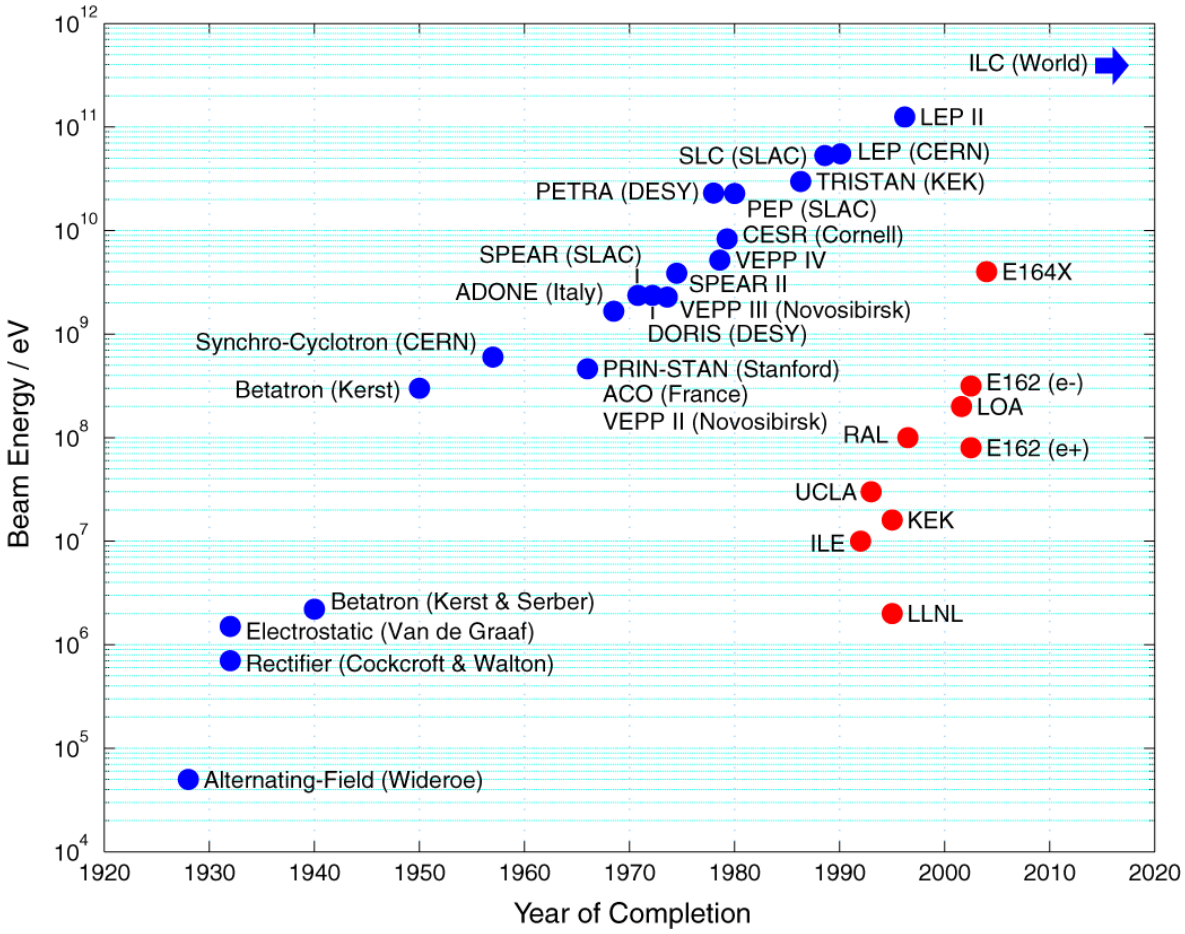

Figure 1: The so-called Livingston plot shows the energy achieved by accelerators as a function of the year when they went into operation. Blue dots indicate working accelerators that have made important contributions in physics, while the plasma accelerators, indicated by red dots, are experiments in themselves. While their progress in the last years is impressive, they have not yet been used to deliver a particle beam of sufficient quality to experiments in physics.

The wake is created when the space-charge force associated with the drive particles displaces the plasma electrons. The plasma ions, which are far more massive than the plasma electrons, remain stationary during the time scale of the beam passing through the plasma. Once expelled, the plasma electrons witness the space charge field of the ion column and are pulled back toward the beam axis, which results in a plasma electron density spike behind the center of the bunch (**Figure 2**). The electric field associated with the density spike accelerates the particles at the back of the electron bunch.

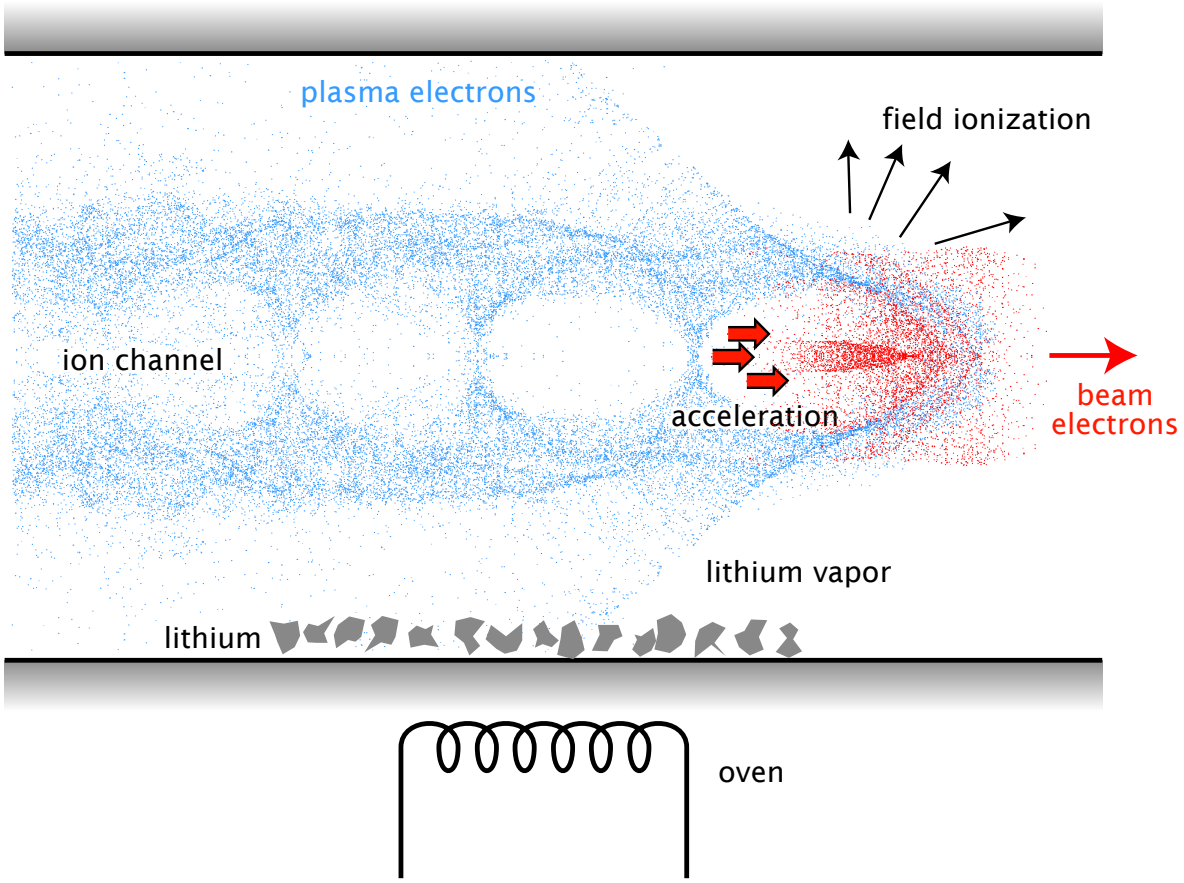

Figure 2: As the relativistic electron beam passes through the plasma, it expels the electrons and leaves behind an ion channel. The wake of the expelled electrons returns to the beam axis; here, the electric field has a longitudinal component that can be used to accelerate electrons in the back of the beam.

Due to their momentum, the plasma electrons overshoot and oscillate about the axis with a wavelength

$$\lambda_p \equiv \frac{2\pi}{k_p} = \frac{2\pi c}{\sqrt{4\pi n_p e^2 / m_e}} \approx 1\text{mm} \cdot \sqrt{\frac{10^{15}\,\text{cm}^{-3}}{n_p}} \tag{1}$$

where n_p is the plasma density. This creates a high-gradient accelerating structure with a wavelength set by the plasma density. The plasma density must be matched to the incoming bunch length, such that the density spike occurs directly behind the bunch:

$$\sigma_{z\,opt} \approx \sqrt{2}/k_p \tag{2}$$

According to linear plasma theory the wake amplitude is

$$eE_{linear} = \sqrt{n_p}\,\frac{n_b}{n_p}\,\frac{\sqrt{2\pi}k_p\sigma_z e^{-\frac{k_p^2\sigma_z^2}{2}}}{1+\frac{1}{k_p^2\sigma_r^2}} \tag{3}$$

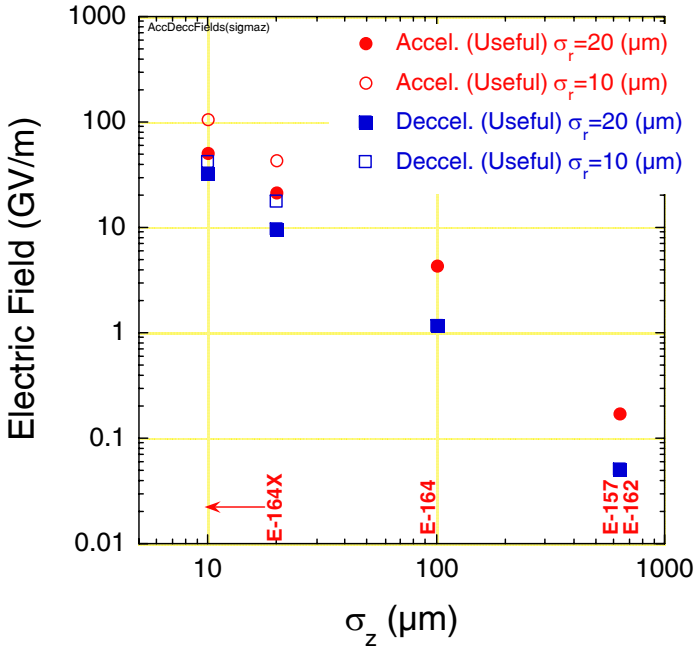

Figure 3: The accelerating field that can be obtained in a plasma, as a function of the length of the drive bunch, as predicted by simulations. The plasma density was chosen according to Equation (2). Bunch lengths on the order of 12μm have been obtained in the FFTB.

with a beam density n_b. For $k_p\sigma_r \ll 1$, and using the optimum bunch length from Equation (2), the accelerating field can be expressed as

$$eE_{linear} = 240\text{MeV/m}\cdot\left(\frac{N}{4\cdot 10^{10}}\right)\left(\frac{0.6\text{mm}}{\sigma_z}\right)^2 \qquad (4)$$

where N is the number of particles in the electron bunch and σ_z is the rms bunch length. For the present setup, $n_b > n_p$, therefore the wake excitation is nonlinear and the above theory does not apply. Nevertheless, numerical simulations have borne out this scaling $E \propto 1/\sigma_z^2$ (see **Figure 3**).

If the current density is high enough, the plasma can be created by the Coulomb field of the relativistic electron bunch. With sufficiently short bunches, the ionization is accomplished by the leading particles of the bunch, such that the majority of the bunch encounters a fully ionized plasma (see **Figure 4**).

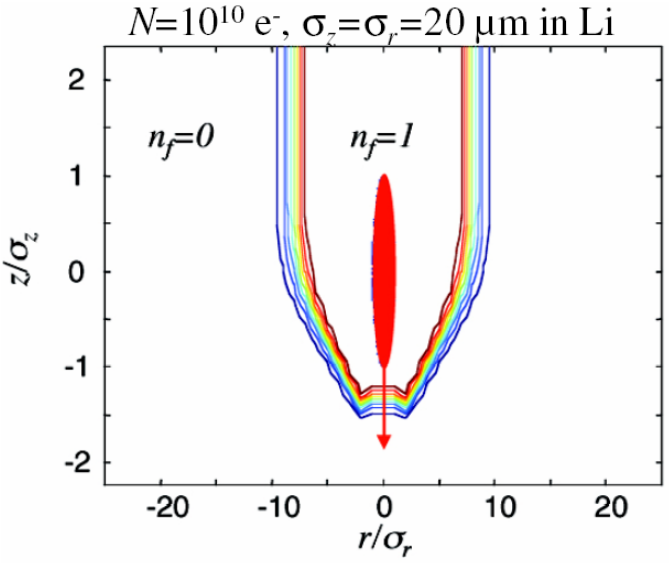

Figure 4: Ionization contours for a gaussian beam calculated using ADK theory. The electron beam is shown in red. The fractional ionization is noted as *nf*. The contour lines indicate that a full ionization is achieved at a position 1.2σ before the center of the bunch.

These high current densities were achieved in the FFTB, making use of a twofold compression process (see section 3.1). Experiments E-164 and E-164X made use of the higher accelerating fields generated by the compressed bunches, using a matched plasma densitiy.

A result of these experiments is shown in **Figure 5**: some of the particles gain as much as 3 GeV of energy. Such acceleration events have been repeatably observed, and the dependency of the acceleration on the plasma density and on the properties of the electron bunch has been studied.

Table 1 shows the standard operating parameters for the E-164(X) experiments. Highlights of the experiments E-157, E-162, E-164 and E-164X are presented in appendix A. In addition to these beautiful physics results, the collaboration has developed a unique apparatus for studying beam-plasma interactions, described in the following paragraphs.

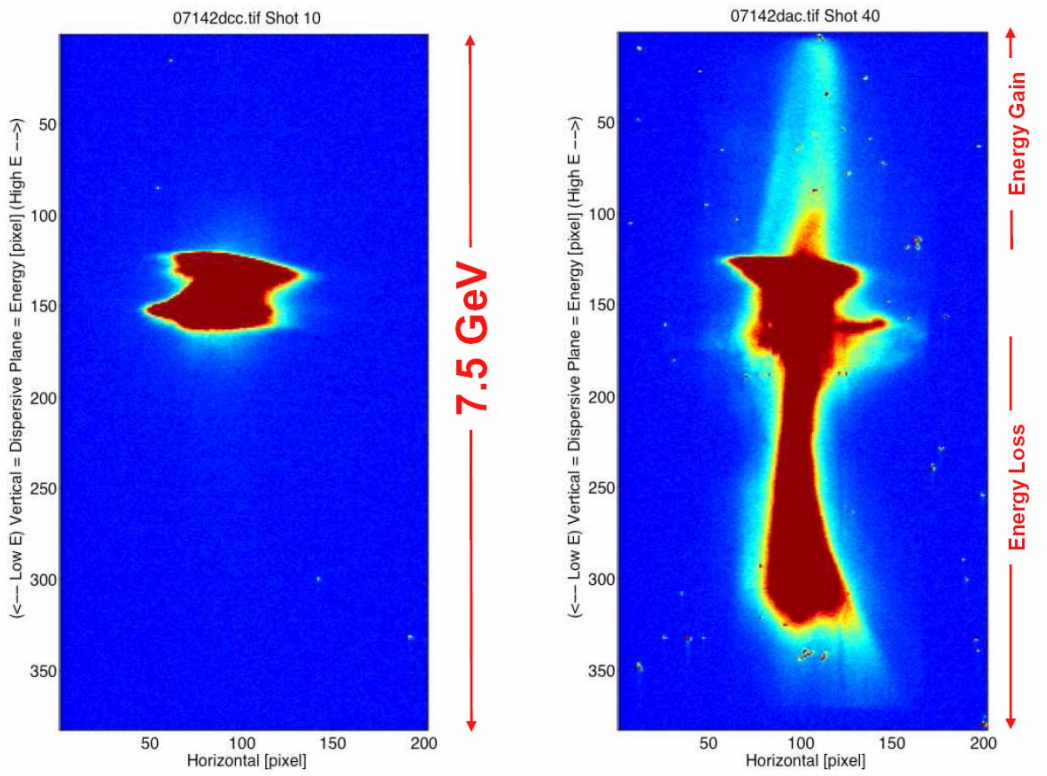

Figure 5: Measurements of the beam in a dispersive plane, without the plasma (left) and with the plasma in place (right). An energy gain of 3GeV is observed.

Table 1: E-164(X) operating parameters in the FFTB.

Mean energy (GeV)	28.5
Energy Spread (full width)	4%
Energy Spread (rms)	1.5%
Bunch Length (σ_z)	~20 μm
Bunch Radius (σ_r)	~10 μm
$N_{electrons}$/bunch	$1.5 - 1.8 \cdot 10^{10}$
Typical Plasma Density (cm^{-3})	$0.5 - 3.5 \cdot 10^{17}$
Typical Plasma Length (cm)	10

3 Existing experimental apparatus

The plasma wakefield acceleration experiments are conducted in the Final Focus Test Beam (FFTB) at the end of the SLAC 3 kilometer linac. The plasma is located just downstream of the FFTB focal point known as IP-0. The complete setup is distributed along more than 100m of the FFTB beamline. **Figure 6** shows the schematic of the experimental set-up for our last experiment E-164X.

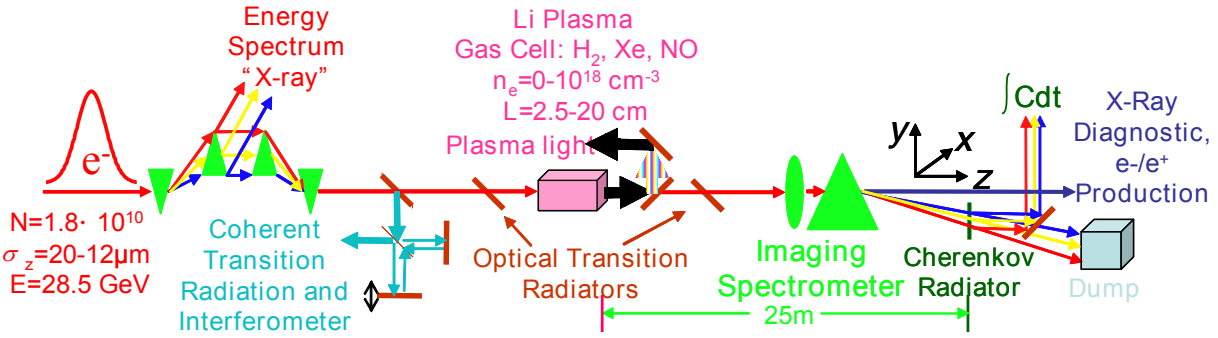

Figure 6: The experimental setup used in the E-164X experiment. Various elements shown in this figure are discussed in the text.

3.1 Beamline

In the summer of 2002, SLAC installed a new bunch compressor chicane for the SLAC linac at the 9 GeV beam energy point (1/3 way down the Linac). Prior to installation of the chicane, the electron bunches had a typical length of 650 μm rms. With the chicane, the bunch is compressed in stages to a predicted minimum of 12 μm. The compression process proceeds as follows (see **Figure 7**). The initially 6 mm long 1.19 GeV bunch in the North Damping Ring is compressed to 1.3 mm in the transition from the damping ring to the linac (RTL). Once in the linac the bunch is given a correlated energy chirp as it is accelerated up to 9 GeV where it is compressed using the magnetic chicane to ~50 μm. In the remaining 2 km of linac the bunch is further accelerated to 28.5 GeV; here, wakefield effects introduce a further chirp which is used in a bend in the FFTB (called "dogleg") to compress the bunches to a length as short as 12 μm (30 fs) rms.

At the entrance to the FFTB, a weak magnetic chicane located in an energy dispersive plane produces a synchrotron radiation stripe with a profile equal to the bunch energy spectrum. The plasma is located near the FFTB focal region known as IP-0. The 28.5 GeV electron bunch is focused to a size of the order of 10 μm rms. The aspect ratio and location of the beam waist are adjusted with the final doublet (quadrupole pair) before IP-0.

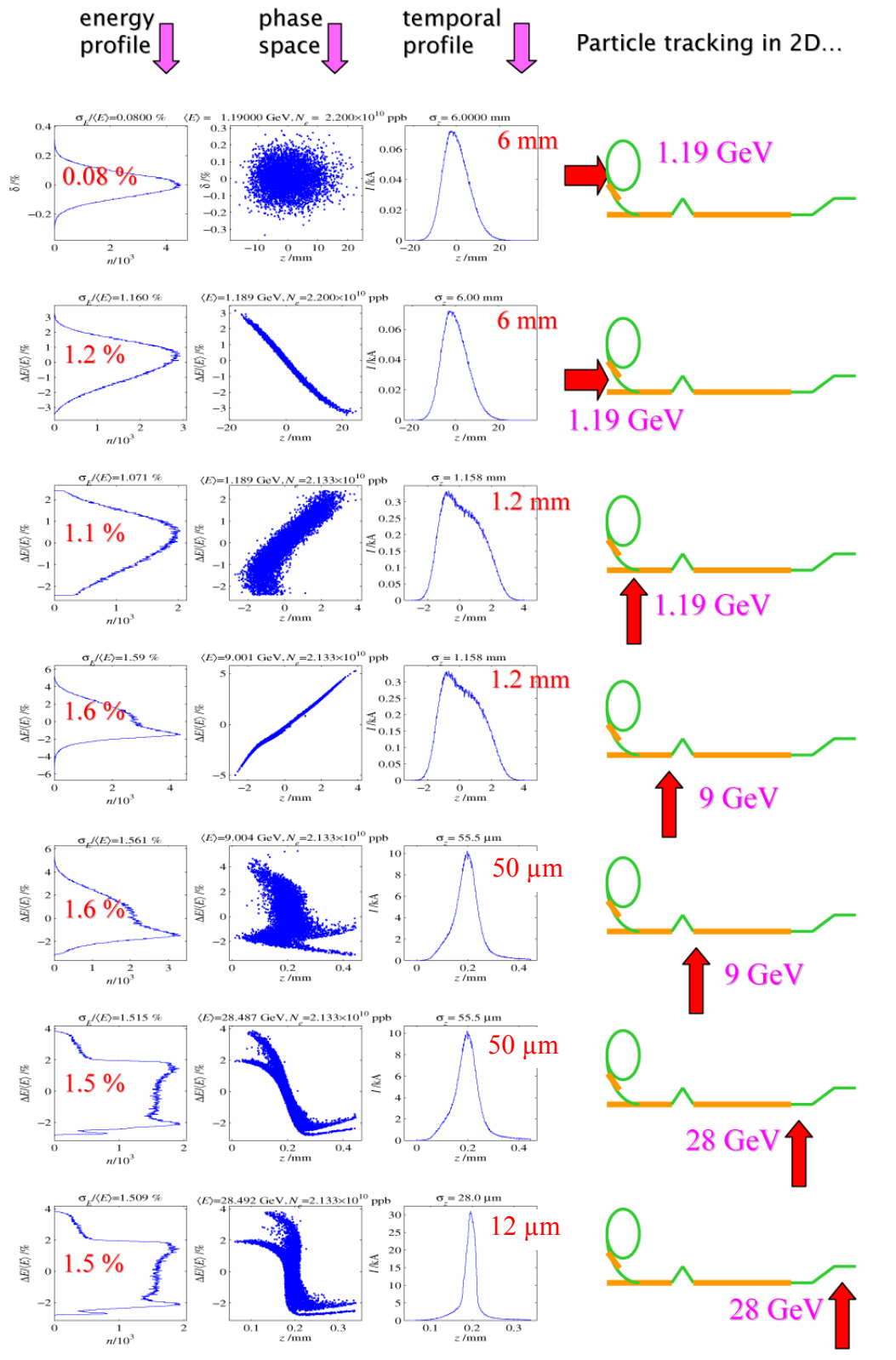

Figure 7: Compression of electron bunches to 12 µm rms. The plots show the development of the longitudinal phase space at different points in the accelerator, simulated using the code LiTrack.

The quadrupoles downstream of IP-0 in conjunction with the FFTB dipole dump magnet form a magnetic imaging energy spectrometer. The spectrometer images the beam exiting the plasma onto a piece of aerogel in an energy dispersive plane. Imaging the beam mitigates the strong plasma focusing and deflecting forces. The transverse profile in the dispersive plane is then an unambiguous measurement of the energy spectrum of the bunch exiting the plasma.

3.2 Plasma source

We have been using an ionized column of lithium vapor (**Figure 8**) as a plasma source with great success for all the previous experiments. Lithium is used for its low first ionization potential, its low cross-section for collisional ionization and its relatively high second ionization potential.

In E-164X, the ultra-short electron bunches required plasma densities of $1\text{–}4 \cdot 10^{17}$ cm^{-3} over 10 cm length. Such high-density plasmas with required axial uniformity cannot be produced in a straightforward manner. We have used the self-fields of the compressed and tightly focused bunch to tunnel-ionize lithium.

As the electron bunch is made shorter to increase the accelerating gradient of the PWFA module, its radial space charge field also increases. For a bunch with a Gaussian profile in r and z, the maximum electric field, measured in GV/m, is given by

$$E_{r\,\max} \approx 5.2 \cdot 10^{-19}\, N / \sigma_r \sigma_z$$

where N is the number of particles in the bunch, and σ_r and σ_z are the rms bunch sizes in the radial and axial directions, measured in meters. This maximum field is reached in the middle of the bunch (z=0), and at $r \approx 1.6\ \sigma_r$. This field can exceed the threshold for field-, or tunnel-ionization of the vapor in which the bunch propagates. The threshold for field-ionization depends on the ionization potential of the atoms ϕ and is of the order of 6.8 GV/m for lithium (ϕ = 5.4 eV). With short bunches the threshold can be exceeded over a large enough volume that the self-ionized plasma is similar to a pre-ionized plasma for the wake excitation.

The fractional ionization created by a σ_r = 15 μm, σ_z = 20 μm bunch with $N = 10^{10}$ electrons is shown in **Figure 4**. The ionization process is essentially a threshold process, and therefore full ionization of the vapor's first valence electron is reached up to $\approx 2\sigma_z$ ahead of the bunch, and up to ≈110 μm radially. For such a short bunch the optimum plasma density for wake excitation, as given by the linear theory, is $\approx 1.3 \cdot 10^{17}$cm^{-3}, and the plasma electrons are expelled to a radius smaller than the plasma radius. A wake amplitude similar to that driven in an infinite pre-ionized plasma can thus be expected in this case. Since the transverse focusing force of the plasma wake allows for the channeling of the electron bunch over many beam beta functions, meters-long, self-ionized PWFA modules may allow for large energy gain in single high-gradient PWFA modules. The self-ionization process could suppress the need for staging of PWFA modules to achieve large energy gains.

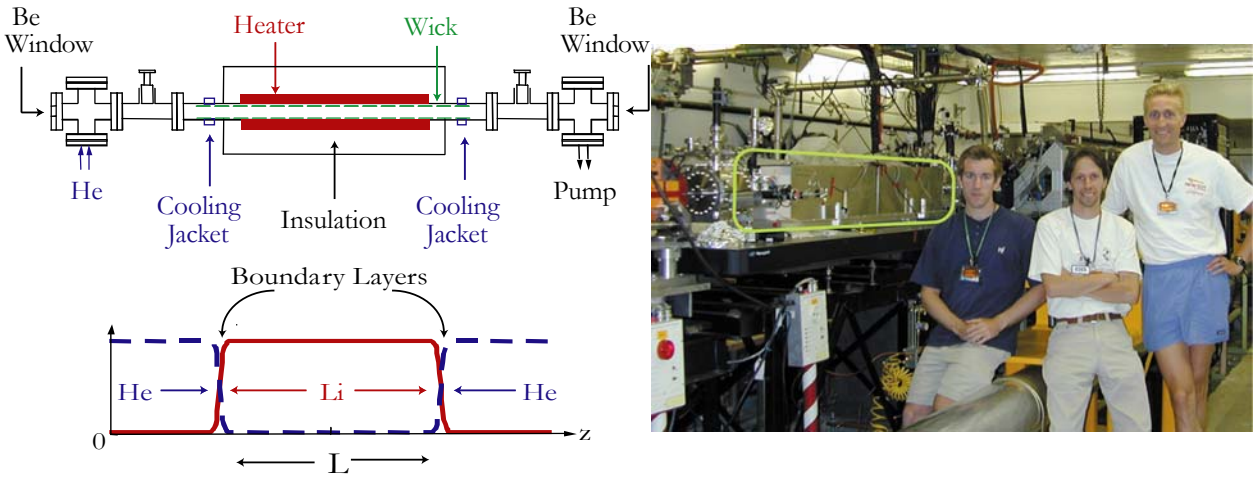

Figure 8: The plasma oven, in a schematic view *(left)* and a photograph of the installed oven *(right)*. A buffer region filled with helium is used to confine the plasma.

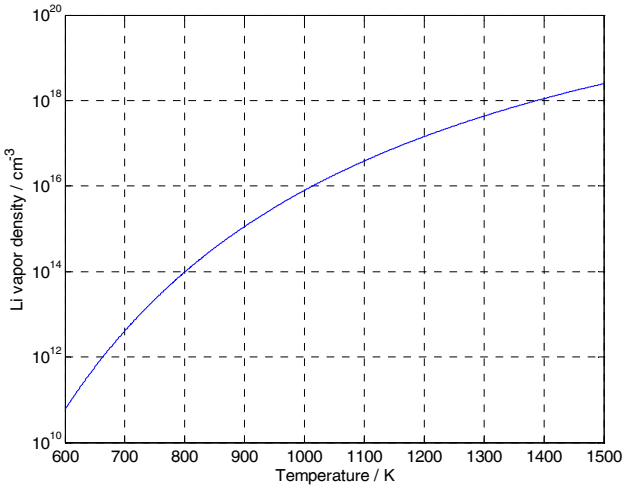

Figure 9: Vapor pressure curve of lithium

In the self-ionized regime, the plasma density is adjusted through the vapor density, which is very stable in a heat-pipe oven, and is insensitive to shot-to-shot changes of the beam parameters. **Figure 9** shows the vapor pressure curve of lithium. A change of temperature from 600 K to 1000 K can lead to a change in vapor pressure density from ~10^{11} cm^{-3} to 10^{17} cm^{-3}. Although it is relatively easy to ionize the first electron of lithium, the second electron has a much larger ionization potential (75.6 eV, ionization threshold of 293 GV/m) which helps to prevent contribution to the plasma density from the ionization of the second electron.

From time to time, it is desirable to have a plasma-off condition. In the past, this was accomplished by turning off the ionization laser. In the beam-ionized regime, this would only be possible by drastically changing the electron bunch parameters. Since this is not desirable, we constructed a pneumatic shuttle system that exchanges the Li oven for a bypass line (a beam pipe filled with the helium buffer gas of the Li oven) in a matter of seconds.

3.3 Diagnostics

In addition to the usual SLC beam position monitors (BPMs) and beam current monitors (toroids), we have developed an extensive set of specialized diagnostics. All diagnostics are acquired at 1 Hz and correlated on a pulse-to-pulse basis.

Incoming bunch energy spectrum

For the compressed bunches, the longitudinal bunch profile is strongly correlated to the energy spectrum. A non-destructive spectrometer following an idea developed for the SLC [6] is used to determine the energy spectrum of the incoming bunches (**Figure 10**). In a horizontally dispersive section at the beam entrance into the FFTB, a weak magnetic chicane deflects the beam in the vertical direction and produces a stripe of beam synchrotron radiation. The horizontal profile of this radiation is the energy spectrum of the incoming bunch. It is measured on a fluorescent Ce:YAG crystal with a cooled CCD camera with 12-bits of dynamic range. The typical rms energy spread on the beam is 1.5% or ~ 420 MeV whereas the energy resolution of the x-rays on the scintillator is about 60 MeV. Thus the relative longitudinal current distribution of the electron bunch can be measured from shot-to-shot. These energy spectra are also used to infer the bunch current profile (see here after).

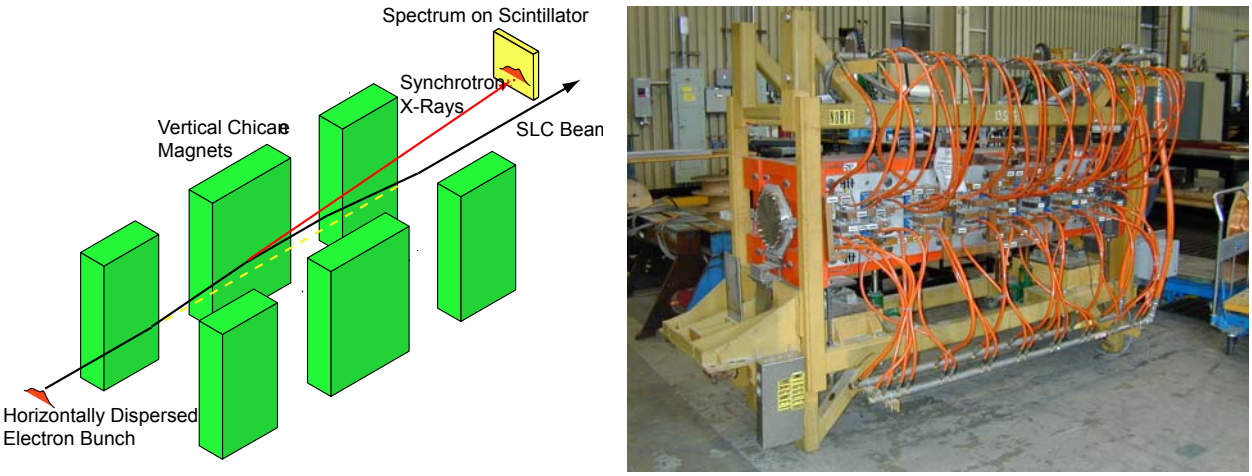

Figure 10: A magnetic chicane, placed in a horizontally dispersive section, is used for a non-invasive measurement of the energy spectrum of the bunch. *Left:* schematic drawing, *right:* the magnets, before the installation.

Bunch length measurement using CTR

When the electron bunch passes through a conducting foil it gives off transition radiation. At wavelengths longer than the bunch length, the radiation is coherent. The total energy of this coherent transition radiation (CTR) is inversely proportional the electron bunch length. The relative bunch length or peak current of each bunch can therefore be monitored by recording their total CTR energy. For our compressed bunches, the radiation is in the THz frequency range and measured with a pyro-electric detector. A Michelson interferometer (**Figure 11**) uses the CTR to produce an auto-correlation trace

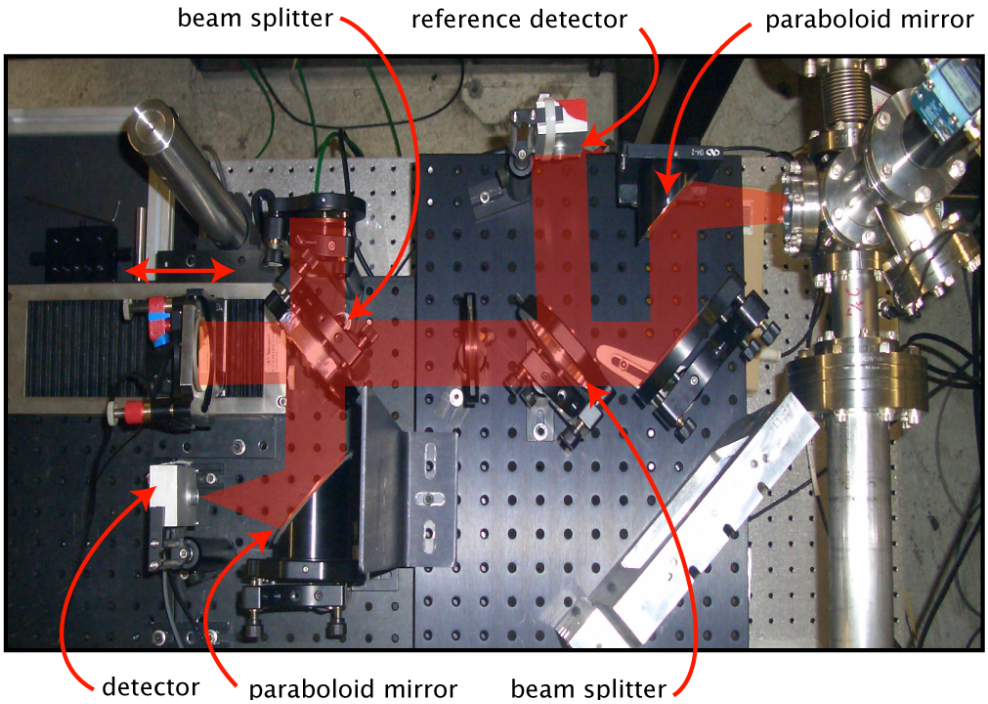

Figure 11: A Michelson interferometer has been set up to record the autocorrelation trace of the coherent transition radiation.

of the longitudinal bunch profile, i.e. an average measure of the electron bunch length (**Figure 12**). The CTR diagnostic is located ≈10 m upstream from the plasma.

Bunch transverse size and position using OTR

The optical portion of the transition radiation (OTR) is imaged onto cooled CCD cameras to measure the transverse profile of the electron bunch ≈1 m upstream and downstream of the plasma. The upstream OTR image provides information about the beam size and transverse profile coming into the plasma while the downstream OTR measures plasma focusing and deflection of the beam. All transition radiators are between 1 and 25 μm thick titanium foils.

Beam energy spectrum after the plasma, Čerenkov radiator

After exiting the plasma, the beam is imaged onto a piece of silica aerogel at IP-2. The visible Čerenkov radiation is imaged onto a cooled CCD camera with 16-bits of dynamic range. The electron bunch vertical profile at IP-2 is dominated by the 10cm vertical dispersion and is the energy spectrum. Thus without the plasma, the current distributions obtained from the Čerenkov can be calibrated against the X-ray chicane. Then when the beam forms and interacts with the plasma, the x-ray chicane image gives us the input beam energy spectrum while the Čerenkov image gives us the effect of the plasma on the beam energy spectrum in the dispersive plane and focusing in the non-dispersive plane.

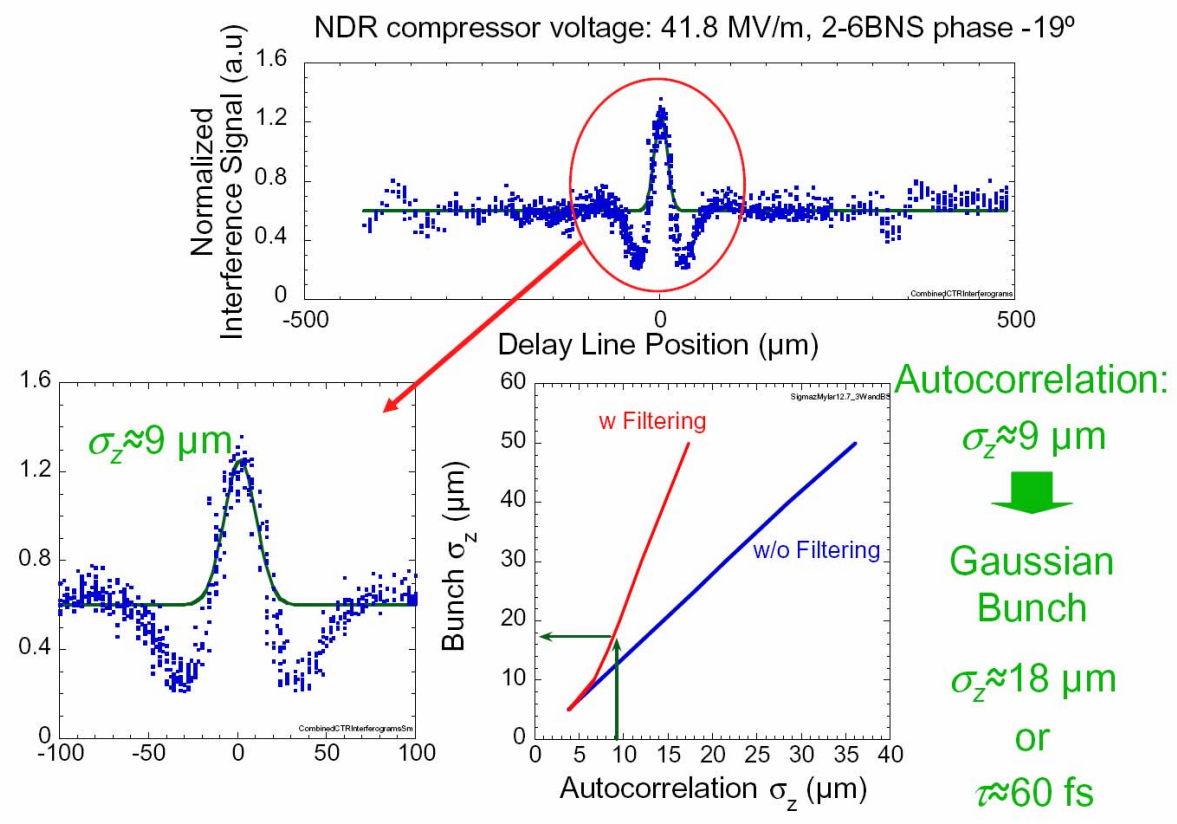

Figure 12: Measured autocorrelation trace of the coherent transition radiation (CTR) that the electron bunch emits when it goes through a titanium foil. The interference is measured with a Michelson interferometer.

Retrieval of the bunch current profile

The achievable electric fields in the plasma depend strongly on the bunch length (or peak current profile), and the amount of charge that is accelerated depends on the electron population in the back of the bunch. However, for bunch lengths in the order of 100 fs, a streak camera does not provide sufficient resolution to measure the longitudinal structure. While the CTR Michelson interferometer can be used to measure the bunch length, its behavior is not well enough understood to yield detailed information on the bunch current profile. Therefore, a different method had to be found to infer the longitudinal bunch shape from other information. The numerical code LiTrack [7] models the development of the z-p_z phase space in the linear accelerator and is therefore used to predict the current distribution and energy spectrum of the bunch for a given setting of the relative phases and compaction factors in the accelerator. However, there are no direct measurements of all the factors, which affect the compression with sufficient accuracy. By comparing the energy spectra that have been measured on the X-ray spectrometer to the ones obtained from the simulation, the accelerator settings can be reconstructed on a shot-by-shot basis and the longitudinal profiles can be inferred. Further comparisons are planned to validate the simulations (see section 6).

Plasma light diagnostics
In this single bunch experiment most of the energy lost by the bunch particles remains in the wake fields and is eventually dissipated in the plasma. A fraction of this energy is emitted in the form of atomic radiation from the excited plasma ions and recombined neutrals. Examining the spectrum of the light emitted by the plasma therefore leads information both on which atomic species is ionized and excited and in a relative sense, of how much energy is deposited in the plasma. This diagnostic therefore provides an independent monitoring of the plasma wake amplitude. It also provides information about possible ionization of the second lithium electron and of the oven helium buffer gas. These ionization processes are possible source for the trapped particles observed in the experiment (see section 4.4 and 4.5).

Positron production
In the plasma, the beam electrons undergo multiple betatron oscillations leading to a large flux of broadband synchrotron radiation. With a plasma density of $3x10^{17}$ cm^{-3}, the effective focusing gradient is approximately 9 MT/m leading to the radiation of photons with critical energies exceeding 50 MeV. This MeV source of broadband X-rays has many scientific applications. The initial application that has been explored is for a positron source, as photo-production of positrons eliminates the thermal stress issues associated with traditional bremsstrahlung sources. Photo-production of positrons has been understood for decades; however, the brightness of plasma X-ray sources provides a unique approach. It is described in section 4.6.

Data acquisition and handling
A distributed computer system has been set up to acquire the large amount of data generated by the experiments. For each bunch, up to five images are stored in addition to the values that the SLC Control Program (SCP) records. For each day of the run, an average of 7.5 GB of data is accumulated.

4 Proposed Next Experiments

The experiments E-157, E-162, E-164 and E-164X have shown that a plasma can sustain very large electromagnetic fields and that this field can be used to accelerate particles over long distances. To pave the road from the proof-of-principle experiments to accelerators useful in other fields of science, several issues have to be addressed:

- it has to be shown that the acceleration can be sustained over longer plasma lengths, increasing the total energy gain
- instead of accelerating a portion of the bunch, a separate bunch has to be accelerated
- the emittance of the accelerated bunch has to be maintained

The present proposal addresses the first two issues.

The improvements to the experimental apparatus, detailed in the following sections, will allow both for a broader range in the parameter space and aim to add another degree of freedom in the sampling of the wake by introducing dual bunches. These modifications fit naturally in the existing experimental setup, described in section 3.

In the present setup, the plasma wavelength and the bunch size in all three dimensions are on the same order of magnitude. For this regime, there exists no analytic description of the dynamics of the plasma wakefield; therefore, it has to be addressed by intricate simulations. To validate these simulations, a detailed comparison to experimental results is mandatory.

4.1 Increased Energy Aperture

With the setup used in experiment E-164X, the maximum energy gain that is possible in the FFTB has been reached. Indeed, in **Figure 5**, one can observe a clipping of the beam energy spectrum both at low and high energy which limits the energy gain and loss to about 4 GeV each. In fact, the limiting elements are located in a short section of the dispersive section of the beamline, shown in **Figure 13**. Replacing the beam tube by one with a larger diameter allows containing a greater spread in particle energies and bringing them safely to the beam dump.

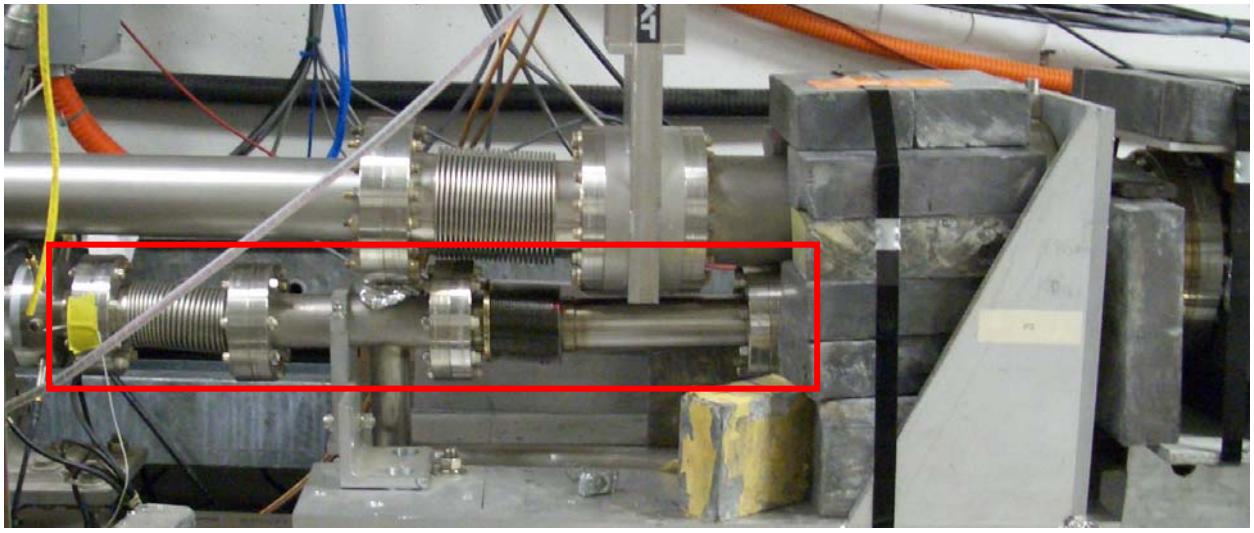

Figure 13: Portion of the dispersive section of the beamline in the FFTB. The upper beam tube is used for the photons produced by the SPPS undulator, the lower beam tube by the electrons. The part indicated by the red box will be replaced by a tube with a larger diameter.

By opening this aperture to accept a total of 20 GeV energy spread in the beam and by increasing the plasma length to 30 cm, we have an excellent chance to achieve 10 GeV energy gain, i.e. to increase the particle energy by one third over only 30 cm! Simulations indicate that this will be possible with a longer plasma (**Figure 14**).

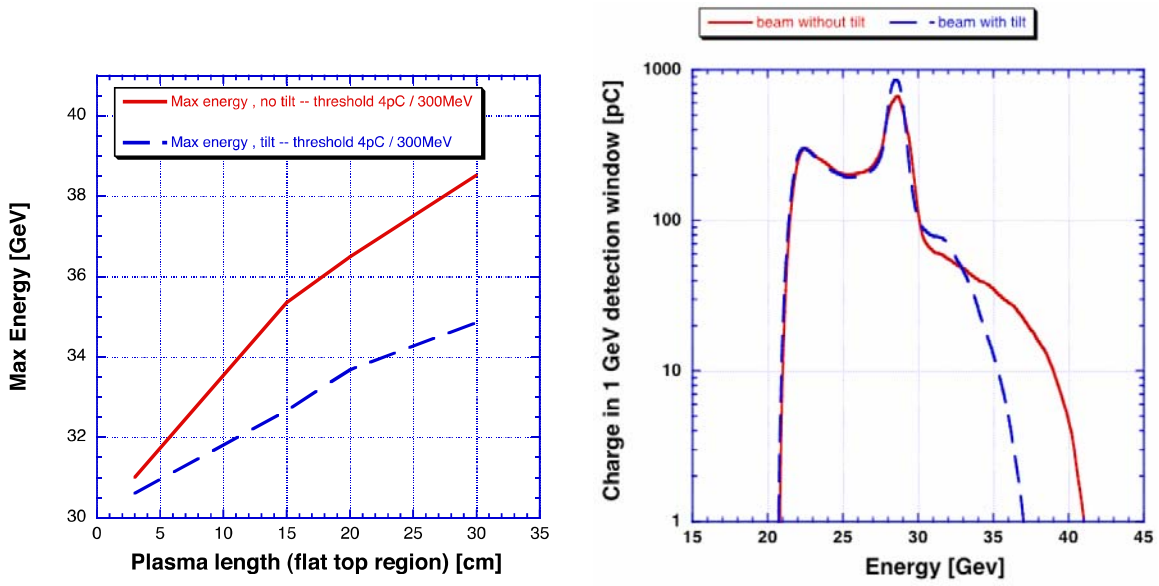

Figure 14: Maximum detectable particle energy, as expected from simulations, as a function of the plasma length *(left)* and the expected energy spectrum after 30cm plasma *(right)*.

4.2 Beam Tilt and Hose Instability Effects

Propagating the beam through a longer plasma seems like a straightforward extension of the E-164X experiment. However, if the bunch enters the plasma with a longitudinal tilt (transverse displacement from front to back), the accelerated particles will "betatron oscillate" in and out of the high accelerating region of the wake located near axis, resulting in a lower energy gain than for a straight beam. The incoming beam tilt can also be amplified or even grow from noise through the hose instability. The effect of transverse oscillations on the energy gain along the plasma is shown in **Figure 15** for both the case of an initially un-tilted beam, and with an initial tilt. In the E-164X experiment, the maximum predicted transverse displacement of a slice 70 μm behind the peak of the beam with no incoming tilt was far less than the transverse spot size of the beam and was thus undetectable (see **Figure 15**). When the plasma length is increased from 10 to 30 cm, the number of beam envelope oscillations increases and the displacement may be detectable.

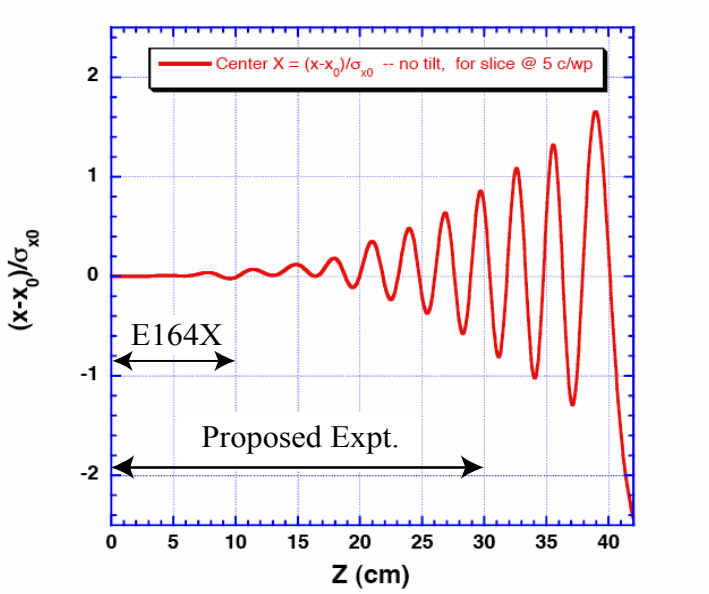

Figure 15: The hose instability can occur as the beam propagates through a long plasma. This could be observed in the planned experiment. This simulation shows the predicted oscillation amplitude in units of the transverse beam dimension as a function of the plasma length.

4.3 Dual Bunch Scheme

Previous experiments have used the head of the electron bunch to create the plasma and excite a wake. Particles in the back of the bunch were then accelerated, depending on their phase with respect to the wake. As a result, one observes a distribution of the particles in energy.

For the PWFA scheme to be applicable to a future linear collider, a real bunch of particles needs to be accelerated to a narrow energy spectrum. This can be achieved by using two bunches, a high charge driver bunch that would create the plasma, drive the wake and loose energy, followed by a lower charge witness bunch that would ride the wake and gain energy. The typical distance between the bunches is of the order of one hundred microns. In the two-bunch scheme, a narrow energy spectrum of the witness bunch can be achieved, while the witness bunch incoming emittance is preserved because the plasma focusing force is constant along, and varies linearly across the witness bunch. Availability of two bunches would make it possible to study the plasma wakefields in detail by varying the two-bunch charge and delay.

A proof-of-principle experiment to demonstrate the acceleration in a dual bunch can be carried out in the FFTB. The suggested approach is described in the following paragraphs.

In the chicane in Sector 10, there is an intrinsic dependency between the horizontal position and the energy of the particles. The energy, in turn, is related to the longitudinal position of the particles through the off-crest acceleration scheme used for the bunch compression. Thus, one obtains the distribution shown in **Figure 16**.

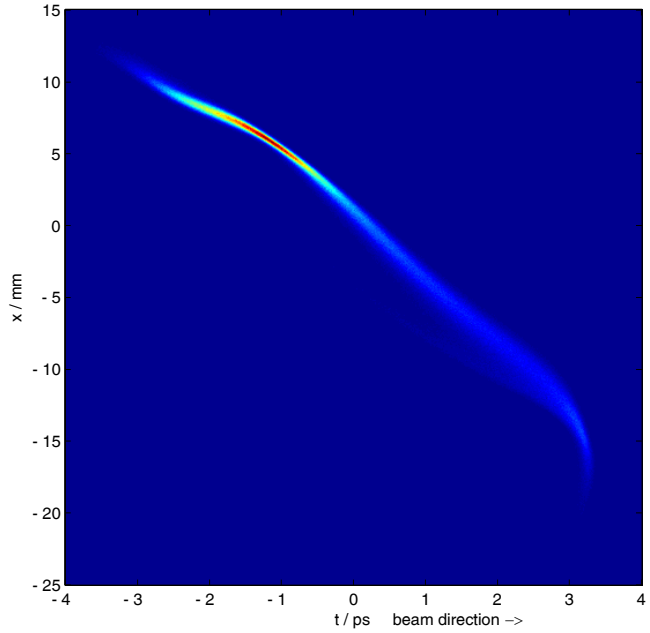

Figure 16: In the middle of the chicane, the transverse position of the particles depends on its energy. Since the beam has an intrinsic time-energy relation, the transverse position x depends on its time t. The rms energy spread in the chicane at the beginning of the linac is 1.2%, in the middle of the chicane it is 1.6%. The simulations have been done using Elegant.

A notch collimator, introduced between the chicane magnets, could be used to create a dual bunch: an absorber that is a few millimeters wide and about one radiation length thick is positioned such that it cuts out a fraction of the bunch (see **Figure 17**). It reduces the energy of the affected particles through bremsstrahlung and spoils their emittance; they get lost in the subsequent part of the accelerator.

Simulations using the code Elegant [8] have addressed the curvature of the energy chirp, the energy loss of the particles through bremsstrahlung, as well as wake field effects of the dual bunches in the oncoming accelerator cavities. The resulting phase space distributions along the accelerator are shown in **Figure 18**. The first bunch is expected to have a peak current of about 10kA, intense enough to field-ionize the lithium vapor and produce a wake in the plasma (see **Figure 19**).

A detector that images the optical transition radiation (OTR) of a thin metallic foil will be installed in the chicane. This will allow matching the simulations of the beam transport with the actual longitudinal distributions. Due to the high radiation background in the accelerator housing, a system of mirrors will transport the OTR light up to the klystron gallery, where a telescope will be used to create an image on a CCD. Special care has to be taken to align the foils and the mirror, since the opening angle of the radiation is only 0.1 mrad. The optical resolution of such a system is currently being studied.

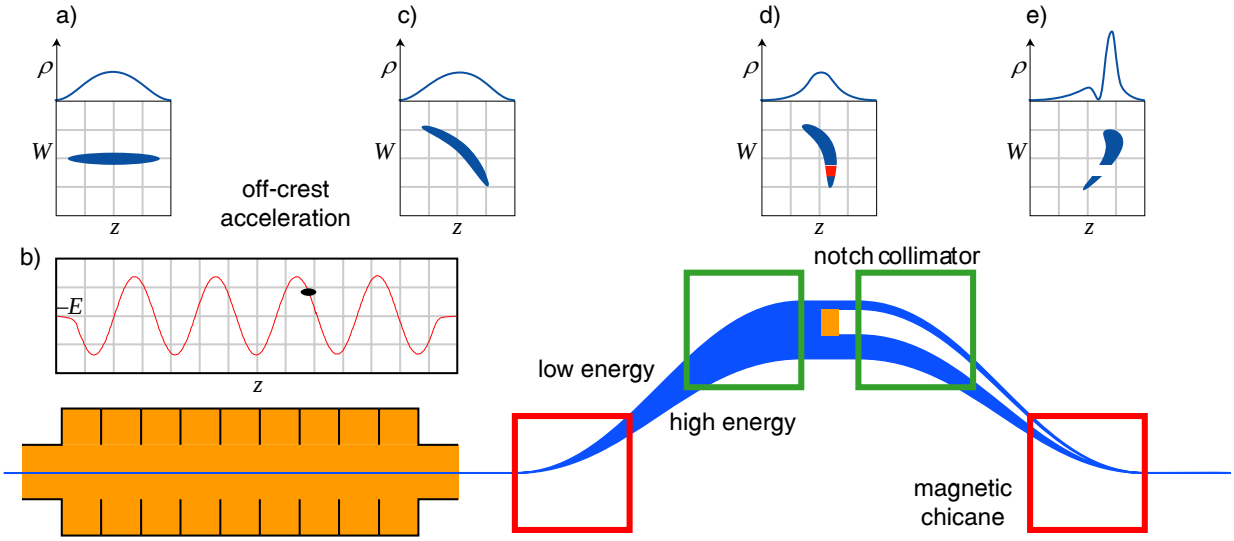

Figure 17: A notch collimator, introduced in the middle of the chicane, removes a portion of the beam. In the following two magnets, the phase space is sheared and the two parts end up separated in time. (The graphs are illustrations.)

Initial calculations indicate that it is possible to create dual bunches in the FFTB using a notch collimator in the middle of the Sector 10 chicane. The profile of the notch collimator and its dimensions and material are being optimized using numerical simulations of the particle trajectories. While copper seems a good choice, both for its thermal properties as well as from the standpoint of radiation protection, other materials are being considered. Particle tracking codes are also used to indicate where the scattered particles are lost.

The technical realization of the notch collimator setup requires one or more motors to move the spoiler and a water cooling system to dissipate the deposited energy. The setup will be designed such that the collimator can be completely removed from the beam path.

Producing dual bunches necessitates running off the phase for maximum compression, because they would otherwise overlap in time. While the second bunch is narrow in energy spread, it will have a considerable extension in time. This is due to a combination of non-linearities in the compression and longitudinal wakefields. Therefore, more intricate collimator silhouettes that may offer the possibility of reducing the length of the second bunch are being investigated.

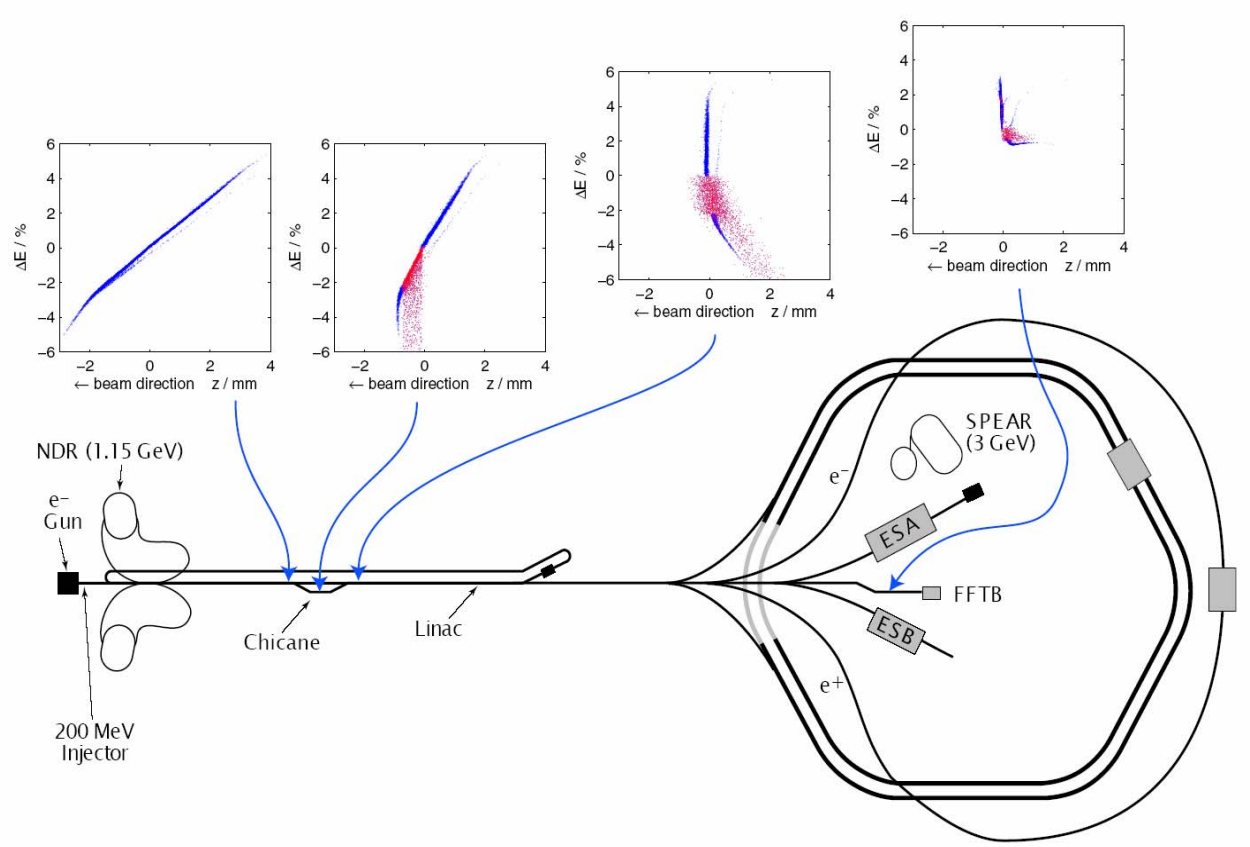

Figure 18: Six-dimensional simulations show the evolution of the phase space in the linear accelerator. The scattered particles are shown in red and may be removed by collimation.

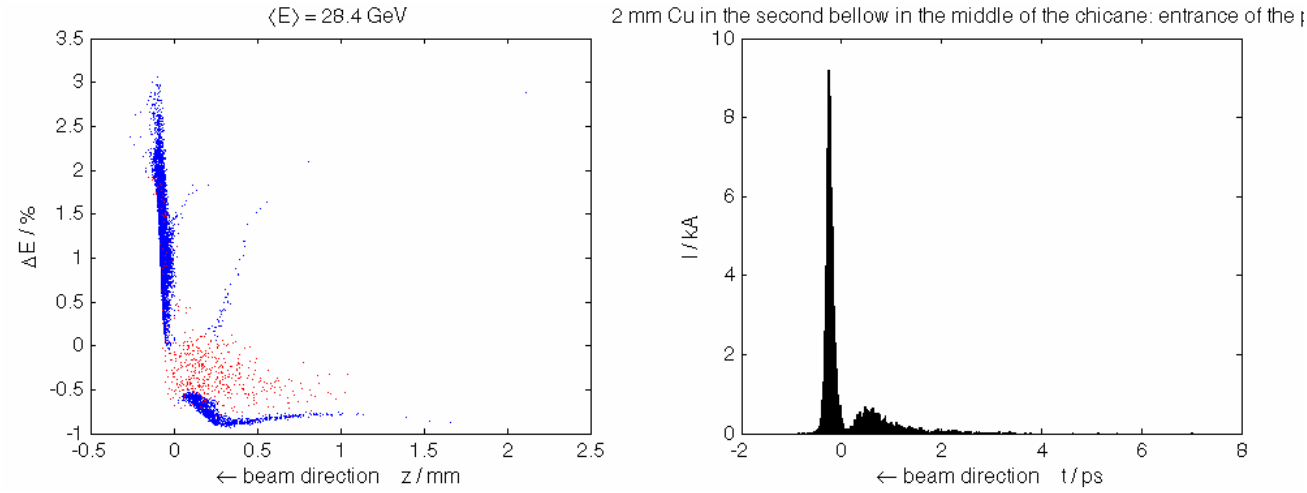

Figure 19: The simulated current distribution at the entrance of the plasma.

4.4 Detection of Fast Ions

An interesting phenomenon is expected once the drive electron beam traverses the dense plasma in the proposed experiment—the generation of fast ions in the few to hundreds of MeV range. There are two distinct reasons for this to occur. The first is the radial explosion of the field-ionized plasma. This extremely narrow but long column of plasma initially has coherent oscillation energy of the wake that is left behind by the beam. However, this energy is rapidly randomized by phase mixing and the plasma electrons begin to move radially outward. This radial expansion of the electron species gives rise to a space charge field, which then accelerates ions. If the average electron energy is on the order an MeV we expect the ions to have roughly Z times the energy which is also about an MeV. This radial Coulomb explosion has been seen in self-modulated laser wakefield experiments where ions with energies on the order 10MeV have been observed.

A second source of fast ions, one that is of particular interest to us, is that related to the acceleration of self-trapped electrons in the plasma wakefield. There are at least three processes that lead to self-trapping of electrons. These are: a) production of Li^{2+} ions by collisional ionization induced by returning electrons produced and blown out by the beam; b) ionization of helium in the downstream lithium to helium transition region; and c) highly localized ionization of Li^{1+} to Li^{2+} wherever the drive beam pinches to a small spot size. These electrons are subsequently self-trapped and accelerated to tens to possibly hundreds of MeV and eventually leave the plasma together with the beam. The sheer numbers of these self-trapped particles can be extremely large (on the order the number of particles in the beam). As the self-trapped electrons leave the plasma column, a space charge field is set up which will pull the ions from the boundary. Many of these ions will be ejected also in the forward direction with similar energies but a far greater divergence angle since they are not relativistic.

It is this group of fast ions we wish to measure. In the last E164X run we installed a prototype Faraday cup that gave some tantalizing evidence for the existence of fast ions. However, the collector foil was not thick enough to stop ions in the tens of MeV range. This Faraday cup is being refurbished to attenuate Li and He ions with energies of up to 100MeV. We also plan to install a fast integrated current transformer roughly one meter downstream of the plasma. The passage of the beam plus the self-trapped electrons will be followed by the fast ions several nanoseconds later. This will induce a current, which has a bipolar signature. If these diagnostics give good results, we will field cellulose nitrate film package for the direct detection of ion tracks and the identification of ion species.

4.5 Trapped Electrons

During the acceleration experiment a number of measurements indicated the possibility that the total charge which exits the plasma is larger than the incoming bunch charge when the electron bunch length is made shorter and shorter (and at the same

time the peak current larger and larger). These measurements include an excess of charge as measured by a toroid located about 70 cm downstream from the plasma, the emission of light with a continuous spectrum on top of the spectral lines of the first ionization state (Li I), and a large excess of light on the downstream OTR foil. In these measurements the amount of charge or light is larger with shorter, higher current bunches.

For the PWFA experiment lithium (Li) was chosen for the plasma because the first Li electron is relatively easy to ionize (ionization potential ϕ_{LiI}=5.39 eV), while the second electron is relatively difficult to ionize (ϕ_{LiII}≈75.64 eV). As stated earlier, field ionization of the Li vapor by the large space charge field of the SLAC ultra-short bunches was used to create the high-density plasma ($<4 \cdot 10^{17}$ cm^{-3}) over distance longer than 10 cm. The Li vapor is confined to the hot zone of a heat-pipe oven by a helium (He) buffer gas filling the beam line at both ends of the oven. To allow for the plasma wake to be driven by the bunch, the Li vapor must be ionized early in the bunch, and up to a radius larger than the plasma collisionless skin depth. The acceleration results show that these conditions were satisfied. However, as the bunch is focused by the PWFA ion column the electric field near the bunch axis increases and Li could be ionized to its second level (Li II). For the same reason, the He in the He—>Li and Li—>He transition regions of the vapor source can also be ionized. These new plasma electrons are born within the accelerating structure of the PWFA and could be trapped and accelerated by large wake fields. This trapping from subsequent ionization is a by-product of the creation of the plasma by the beam itself.

Trapping of plasma electrons is equivalent to the dark current of RF accelerators and can create unwanted, low energy particles in the accelerator. Depending on the number of trapped electrons and on the energy they acquire, these electrons could load the plasma wake and therefore degrade the quality of the accelerated beam, or even reduce its energy gain. It is therefore important to understand their origin and characteristics. Unfortunately, an energy measurement by a time of flight method is not possible with relativistic electrons. We therefore want to carefully correlate the number of trapped particles with the acceleration signal, as well as with the bunch characteristics. We also want to identify the source and the mechanism for the trapping using systematic numerical simulations of the PWFA with realistic plasma boundaries including the He gas. Simulation codes that include the ionization and that can model the full-scale experiment in a reasonable amount of time have recently been developed by our collaboration. Preliminary results seem to indicate the trapping of electrons from both the Li and the He, with energies in the 10-100 MeV range.

4.6 Positron Source from Betatron X-rays Radiated in a Plasma Wiggler

There is a large flux of synchrotron radiation that is a by-product of the plasma wakefield experiment, and it creates an opportunity that should not be neglected. For example, it could find application as a positron source. We measured the 14 keV flux

during E-157 and have made preliminary measurements of the pairs produced by the much higher energy gamma rays during E-164X. We are now proposing to build on these positive results.

Using the parameters listed in **Table 1**, the effective focusing force, the wiggler strength of the ion column and the resonant frequencies of the radiation can be calculated. When the wiggler strength $K>>1$, as in our case, higher harmonic radiation is generated, and the spectrum of individual electrons at different radii within the bunch will overlap creating a broadband spectrum. The results are listed in **Table 2**.

Table 2: Typical Betatron Radiation Characteristics of the Electron Beam Parameters Listed in Table1.

N_p (cm^{-3})	B_{eff} (T)	K	E_c (MeV)	Photon Beam Divergence (mrad)	Energy Loss dE/dz (GeV/m)	Number of Radiated Photons per Pulse
$3.0 \cdot 10^{17}$	90	173	49.6	3.09	4.3	$1.31 \cdot 10^{11}$

At this typical plasma density, we have an effective magnetic field strength of 90 T. Perhaps more startling is the fact that a r_o=10μm electron loses about 430 MeV in only 10 cm while radiating nearly 10 photons with a critical photon energy of nearly 50 MeV.

The pair production experiment takes place nearly 40m downstream of the IP0 plasma. Since the characteristic photon beam divergence is large, ~ K/γ, collimators are used to create an 8 mm dia photon beam for particle spectroscopy. This beam hits a high-Z target to create pairs, and particles up to 27 MeV are imaged in a magnetic spectrometer. They are detected using silicon surface barrier detectors and by imaging a phosphor that resides on the particle image plane using an intensified camera. Several positive results were obtained during E-164X. There was clear evidence that the spectrometer was imaging the converter target and that the fluxes of positrons and electrons were equal. Both of these give us confidence that a real signal can be observed in a high background environment.

The following upgrades are being planned for this proposed experiment. First, a pole piece is being manufactured that will allow us to *simultaneously image* both particle polarities. This will allow us to verify that the electron and positron signatures are the same on an individual shot basis. A schematic of the design is shown in **Figure 20**. Second, additional collimation will be added to reduce the background from particles that scatter to large angles after they are produced. An electromagnetic shower code (EGS) is being used to design the collimation and to choose the optimum converter thickness and material. Finally, a Čerenkov diagnostic will also be employed as a threshold detector.

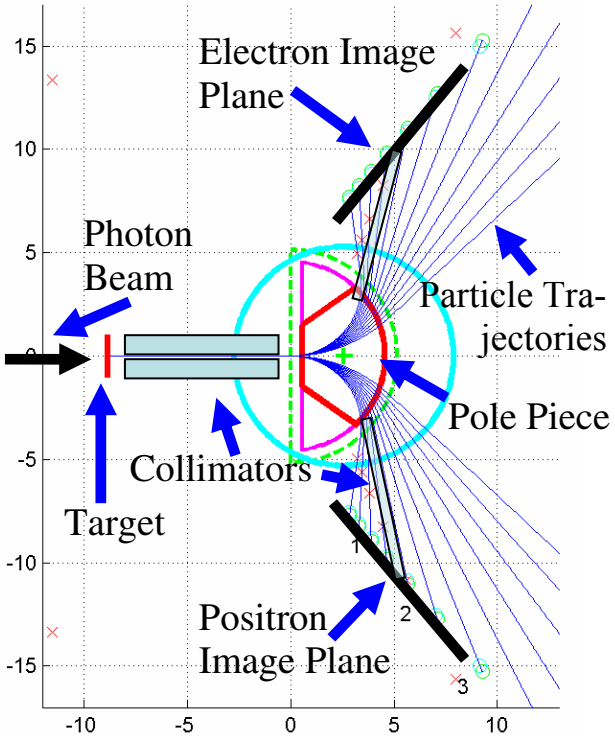

Figure 20: Schematic of the Upgraded Magnetic Spectrometer Design

4.7 New and Improved Diagnostics

The experimental results summarized in section A were made possible by the continual development of specialized diagnostic tools: Optical Transition Radiation (OTR) profile monitors, time-integrated and time-resolved Čerenkov light profile monitors, non-invasive energy spectrometers, and broad-band terahertz power meters to monitor CTR radiation to name a few. These have been developed to quantify the inner structure of the bunch, which depends critically on the stability of various accelerator components. For example, the bunch length is influenced dramatically by modest phase changes in the accelerating cavities: if the bunch has its shortest possible length in the FFTB (~12 μm rms), an RF phase error of 0.5-degrees S-band in the sectors 2-6 of the linac induces a relative bunch length change of 15%, with the chicane energy feedback switched on.

The experiments listed in the previous sections will benefit from additional diagnostic capabilities. Of the three stages in the bunch compression process, the compression in the sector 10 chicane is proportionately the largest. Further, successful creation of the dual bunches requires matching an appropriate collimator width and location with the appropriate energy spectrum. For these reasons, we will upgrade an existing (but not functional) OTR screen in the middle of the chicane to provide detailed energy spectra in the middle of the chicane on a pulse-to-pulse basis.

Data with the plasma source in the beamline is acquired at a rate of 1Hz. Tuning up the linac to give the optimally compressed pulses with good transverse emittance is

more readily accomplished at 10Hz. Many of our diagnostic CCD cameras are cooled for a high dynamic range to help us monitor subtle details of the beam profile or spectrum. Although very sensitive, these cameras have mechanical shutters which prevent them from working reliably at 10Hz. We are in the process of upgrading several of our cameras to models with electronic (not mechanical) shutters that can monitor the beam at 10Hz and aid in tuning up the beam.

To date, the only direct measurement of the ultra-short bunches has been through a THz autocorrelator constructed during the E-164X runs. At maximum compression, the electron bunch profile is nearly Gaussian and symmetric. Much of the plasma data is taken with the beam deliberately not at maximum compression when the beam is predicted to have an asymmetric shape consisting of a relatively long low-current 'trunk' or 'tail' and a high-current relatively symmetric central core. The autocorrelation of the beam pulse is an inherently symmetric function and thus will not provide detailed information about the longitudinal pulse shape. However, it is a relatively simple diagnostic, which provides an average measurement of the high-current core of the bunch. The existing autocorrelator is shown in **Figure 11**. The autocorrelation traces show the maximally compressed bunches are in the 10-20 μm rms range predicted by simulations. The dynamic range of this device is currently limited by the THz properties of the materials used for beam windows and splitters. We will investigate the dynamic range of this device with alternate material beam windows and splitters to improve on the dynamic range measured thus far. Finally, we are in the design stages of a more advanced single shot autocorrelator that will use a modified design in conjunction with a segmented detector to make this measurement for each individual bunch.

5 Experimental program schedule

The experiments described in section 4 can be carried out in three runs. A separation of two months between the runs will allow preliminary analysis of the data and improvements to the experimental apparatus accordingly.

Each run should have a length of two to three weeks. Before the first run, an additional week is needed to access the FFTB area and to install the plasma oven and the diagnostics. The installation of the notch collimator for the dual bunch experiment (section 4.3) requires a week of access to Sector 10 of the SLC linac.

6 Cooperation with Other Experiments

The plasma wakefield acceleration experiments have spawned collaborations with other groups at SLAC, mostly in the field of electron beam diagnostics. The development of methods to measure the bunch length and the longitudinal particle distribu-

tion is of particular interest to the Linac Coherent Light Source (LCLS). We cooperate also in the development of optical transition radiation monitors.

A joint experiment with the electro-optical sampling (EOS) is planned in the commissioning of the dual bunch scheme: by measuring the energy spectrum and the longitudinal profile simultaneously and by comparing these measurements to the simulations of phase space evolution in the accelerator, we hope to advance the understanding of this important field.

7 Summary

The planned experimental upgrade to the plasma wakefield acceleration experiment will allow us to measure particles whose energy has been increased by up to 10 GeV over only 30 cm, which is three times more than in previous experiments. Increasing the length of the plasma accelerator will also allow us to study the stability of the plasma wake over a longer distance, which could be affected by hose instability effects.

A proof-of-principle experiment to tailor the longitudinal bunch shape is also planned. A notch collimator, introduced in the beam in the middle of the Sector 10 chicane, will take out a portion of the bunch. This leads to a dual bunch, separated in space. The propagation through the following part of the accelerator transforms this into a longitudinal modulation. The first of the dual bunches will excite a wake in the plasma, the second can be used to sample this wake.

Furthermore, several improvements are planned for the diagnostics of the electron beam: new cameras will provide a higher frame rate, and an improved autocorrelator will improve the measurement of the longitudinal bunch shape.

Appendices

A Highlights of the Experiments

E-157

A.1 Collective Refraction of the Electron Beam at a Plasma-Gas Interface

P. Muggli et al., Nature, Vol. 411, p. 43 (2001),
P. Muggli et al., Phys. Rev. Special Topic-AB Vol. 4, 091301 (2001)

The observation of refraction and eventual total internal reflection of the electron beam as it exits the plasma/gas boundary was among the unanticipated results of E-157. The interface is produced by a well-defined laser beam, which is used to create the plasma via photo-ionization of a column of lithium vapor. The observed refraction is analogous to the usual refraction for a light beam, however the associated "Snell's law" is time-dependent and non-linear.

A physical explanation for this effect is as follows. In the plasma, the electron beam, with density greater than plasma density, has a symmetric focusing force on it because of the expulsion of plasma electrons. However, as the beam begins to exit the plasma the focusing force becomes a deflecting force, bending the beam away from its trajectory toward the plasma. This deflection has been measured as a function of the incoming beam angle and found to be in quantitative agreement (see Figure A.1) with both a model and three-dimensional PIC code simulations of the experiment.

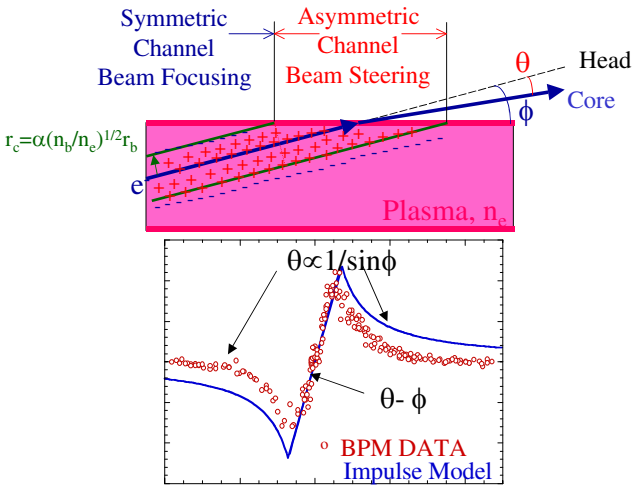

Figure A.1: Cartoon (top) showing the physical reason for refraction of an electron beam at the plasma/gas boundary and the observed angle of refraction as a function of the incident angle ϕ.

A.2 Transverse Betatron Dynamics of a 30 GeV Beam in a Long Plasma

C. Clayton et al., Physical Review Letters, Vol. 88, 154801 (2002).

In the E-157 experiment, the electron beam was not "matched" to the plasma. Consequently, the betatron motion of individual electrons produces multiple oscillations of the electron beam envelope over the plasma length. Thus, the spot size of the electron beam on a screen downstream of the plasma oscillates as the plasma density is increased. In Figure A.2, we show these oscillations measured during E-157 experiment. The solid line is the prediction of a model based on the focusing force on the beam provided by a uniform ion channel. The model has no free parameters. One can see that this model predicts both the densities where a minimum spot size is expected and the amplitude of the oscillations rather well. At the highest densities, there is a breakdown of the model as the plasma density becomes comparable to the beam density and the beam is unable to completely blow out the plasma electrons and establish the ion channel.

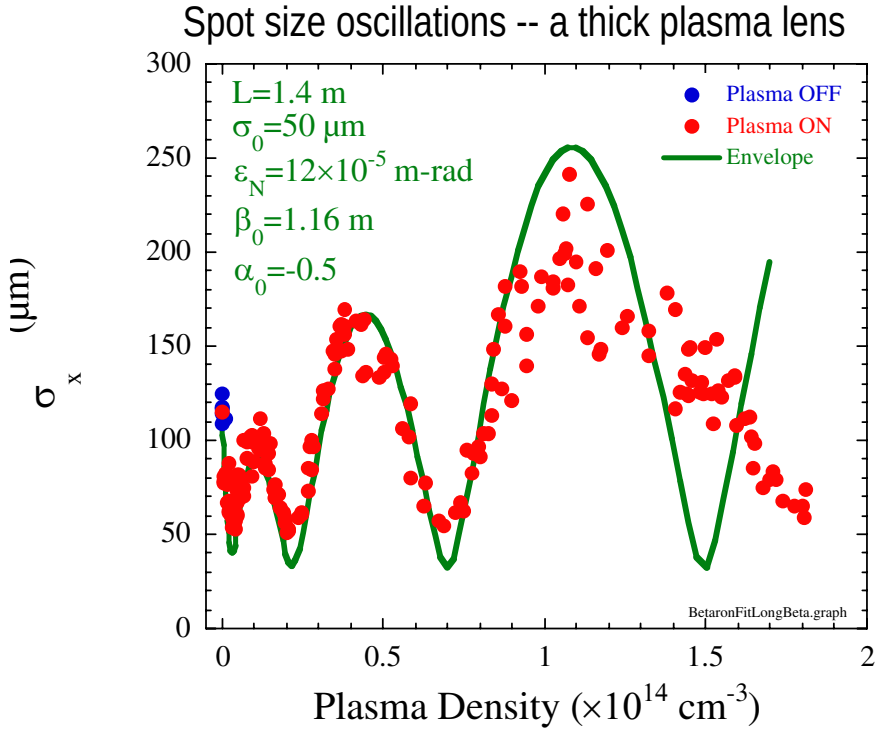

Figure A.2: The observed variation of the electron beam spot size on an external screen as the plasma density is increased in the E-157 experiment.

A.3 Demonstration of a Plasma Wiggler with High Beam Brightness

S. Wang et al., Physical Review Letters, Vol. 88, 135004 (2002).

The betatron oscillation of the beam envelope by the transverse electric field of an ion column results in the generation of synchrotron radiation. Since the beam at SLAC is ultra-relativistic, this emission is strongly peaked in the forward direction. Even though the emission is incoherent and broadband, the peak brightness of the x-ray beam is comparable to the undulator radiation at synchrotron light sources.

In the E-157 experiment, we measured the absolute photon yield, the angular spread and the density dependence of the X-rays. The X-rays were emitted with a divergence angle of 0.1-0.3 mrad, and the x-ray yield varied quadratically with plasma density. The absolute photon yield and the peak spectral brightness at 14.2 keV were estimated to be $6 \cdot 10^5$ and $7 \cdot 10^{18}$ per (second mrad^2 mm^2 0.1% bandwidth). Figure A.3 shows an image of the X-rays on a fluorescent screen placed 40 m downstream of the plasma in the E-157 experiment. A well-defined beam due to betatron x-rays is clearly visible on top of the bending magnet radiation generated as the 30 GeV electron beam is swept out of the way.

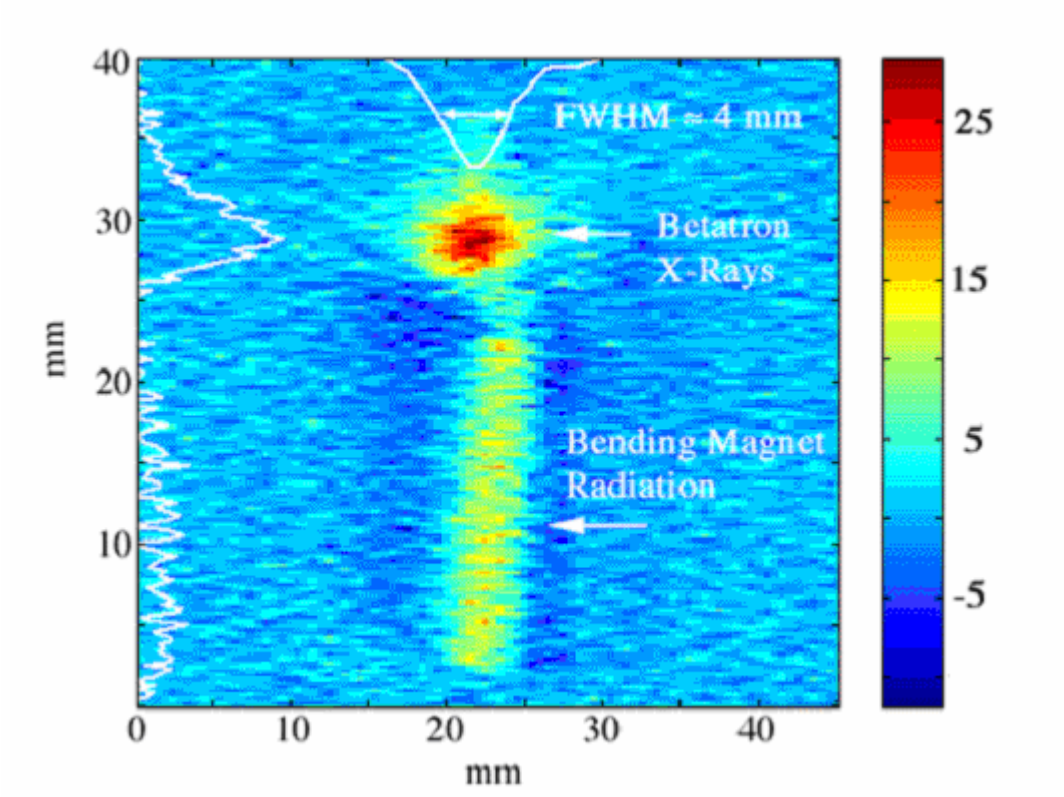

Figure A.3: Betatron radiation emission of X-rays above 6 keV seen in the E-157 experiment.

A.4 Focusing of a Positron Beam

M. Hogan et al., Physical Review Letters, Vol. 90, 205002 (2003).

The mechanism for focusing of a positron beam by a plasma is quite different than that of an otherwise identical electron beam. In the case of a positron beam, the plasma electrons are sucked in from different radii outside of the beam. These electrons arrive at different times and the peak electron density on axis of the positron beam can far exceed the beam density. Thus the focusing force is neither linear in the radial direction nor is it constant in the longitudinal direction as it is in the electron beam case in the "blowout" regime.

We have measured both the time-integrated and time-resolved focusing of the SLAC positron beam as it traverses a 1.4 m long plasma column. The time-integrated measurement was done by measuring the beam size at two different locations downstream of the plasma as a function of plasma density. A maximum demagnification of a factor of two has been demonstrated (see Figure A.4)

The time dependent focusing of the beam has been measured using a streak camera and compared with simulations using the code QUICKPIC. The focusing force is seen to vary in a nonlinear fashion along the full 12 ps length of the positron beam.

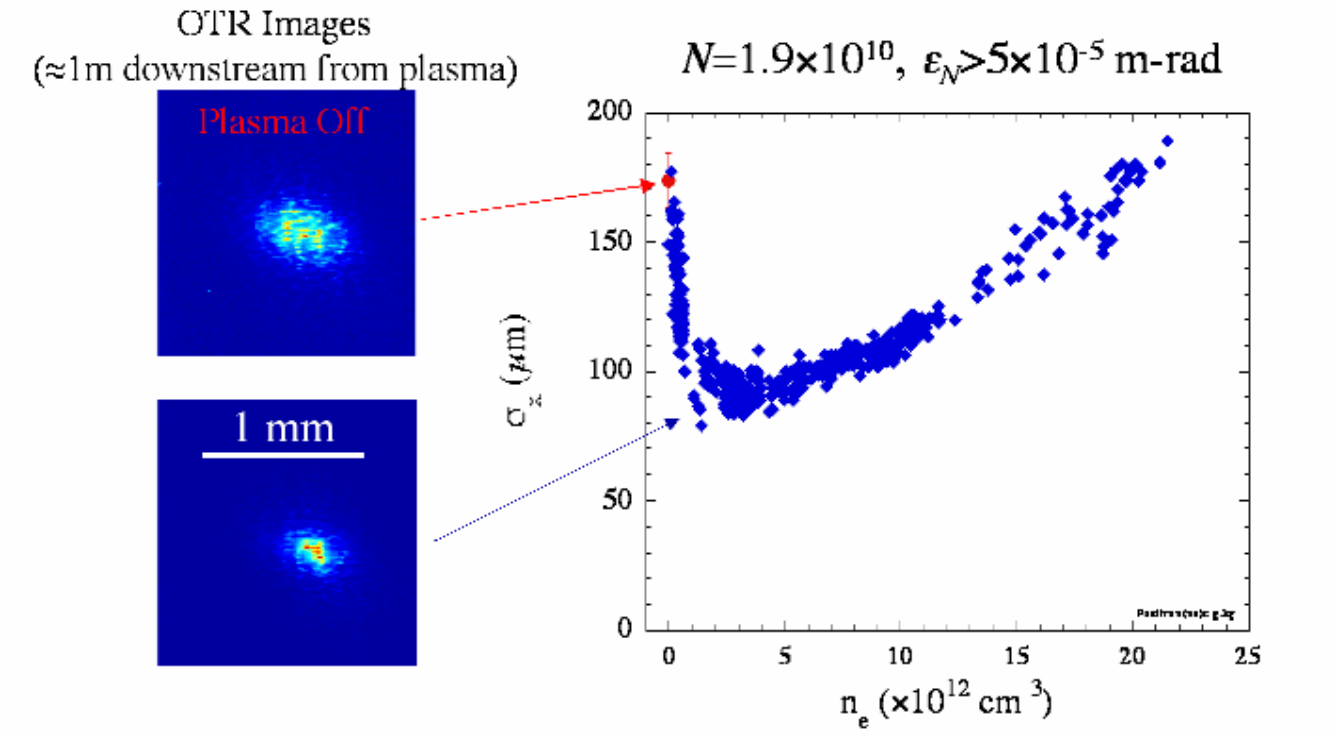

Figure A.4: Focusing of the 28.5 GeV positron beam. The spot size of the positron beam measured on a screen placed approximately 1 m after the plasma as a function of plasma density.

A.5 Dynamic Focusing Within a Single Ultra-Relativistic Electron Bunch

C. O'Connell et al., Phys. Rev. Special Topics-AB, Vol. 5, 121301 (2002).

In the blow-out regime, as the beam propagates through the plasma, the density of plasma electrons along the incoming bunch drops from the ambient density to zero leaving a pure ion channel for the bulk of the beam. Thus, from the head of the beam up to the point where all plasma electrons are blown out, each successive longitudinal slice of the bunch experiences an increasing focusing force due to the plasma ions. The time-changing focusing force results in a different number of betatron oscillations for each slice depending upon its location within the bunch. Since the incoming electron beam has a correlated energy spread, this time-dependent focusing of the electron bunch has been observed by measuring the beam spot size at the Čerenkov radiator, which is in the image plane of a magnetic energy-spectrometer imaging the plasma exit. Each plot in Figure A.5 represents a section in time, where time progresses from left to right, then top to bottom. We see that the number of betatron oscillations within the bunch increases towards the back of the bunch (Figures A.5a-g) but only up to the blowout time occurring approximately at the plot labeled $\tau = 0$ ps (Figure A.5h). Clearly, each successive slice of the bunch, from $\tau = -4.9$ ps to $\tau = 0$, is experiencing a stronger effective focusing force than the slice prior to it. Conversely, the ambient plasma density needed to reach any given minimum decreases with time along the bunch. The locations of the minima are both slice-and density-dependent. Figures A.5i-l are in the blow-out regime as the focusing force is no longer changing.

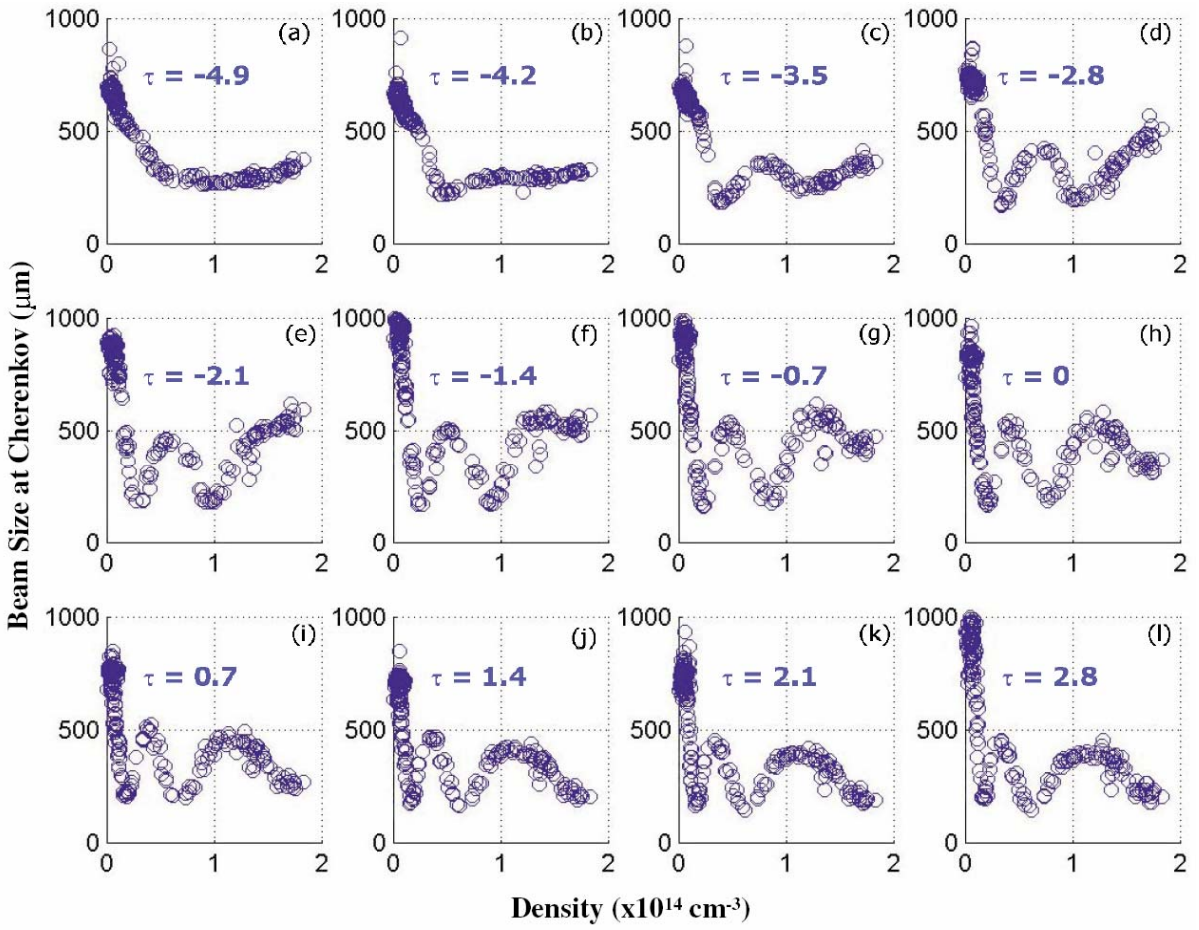

Figure A.5: Individual Čerenkov Time Slices (read L-R, T-B). Graph (a) shows the weak focusing force, which dominates the first head slice. Beginning at graph (b) the slices are in the linear portion of the chirp. Graphs (i)-(l) are in the blowout regime, since the focusing force is no longer changing.

E-162

A.6 Acceleration of Positrons by the Plasma Wake-field

B. E. Blue et al., Physical Review Letters, Vol. 90, 214801 (2003).

High-gradient acceleration of both positrons and electrons is a prerequisite condition to the successful development of a plasma-based e^+-e^- linear collider. Such an accelerator employs the longitudinal electric field of a relativistically propagating wakefield in a plasma to accelerate charged particles. In proof-of-principle experiments, laser-driven plasma wakefields have been shown to accelerate electrons at electric fields that are significantly greater than those employed in current radio-frequency accelerators are.

We have now shown for the first time that a beam of positrons can drive and be used to probe the longitudinal electric field component of the plasma wakefield. When a 28.5 GeV, 2.4 ps long positron beam at the Stanford Linear Accelerator Center containing $1.2 \cdot 10^{10}$ particles propagates through a Lithium plasma of electron density $1.8 \cdot 10^{14}$ cm^{-3}, the main body of the beam is decelerated at a rate of approximately 49 MeV/m, while a beam slice containing $5 \cdot 10^{8}$ positrons in the back of the same bunch gains energy at an average rate of ~ 56 MeV/m over 1.4 m. These results are critical to the development of future plasma based linear colliders. Figure A.6 shows the summary of results on positron acceleration from a paper published in Physical Review Letters.

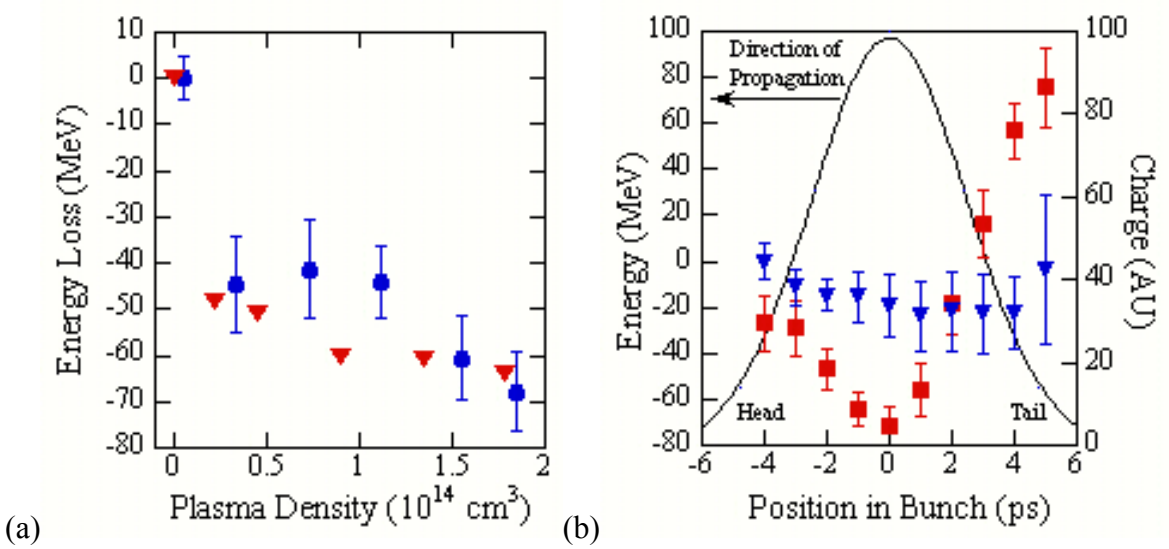

Figure A.6: (a) The energy loss by the center 1 ps slice of the positron beam as a function of plasma density (blue circles) and the prediction from 3D, OSIRIS simulations. (b) The slice-by-slice energy change of the positron beam showing both energy loss in the front half and the energy gain in the back half of the beam for a density of $1.5 \cdot 10^{14}$ cm^{-3}. The red curve is with the plasma on and the blue curve is with the plasma off. The black curve is the positron beam charge distribution.

A.7 Electron Beam Acceleration Using a Matched Beam in a Plasma

P. Muggli et al., Physical Review Letters, Vol. 93, 014802 (2004).

The key to control the transverse effects of the plasma was to propagate a matched beam. In a matched beam the emittance force of the beam balances the focusing force by the plasma and the beam propagates without spreading, i.e., it exits the plasma as it entered it, which makes it easy to image the beam. Figure A.7 shows conclusive evidence for matched-beam propagation. At lower densities, the emittance force of the beam exceeds the focusing force. As the focusing force is increased (by increasing the density), the beam spot size oscillations damp down. Eventually the beam is matched to the plasma.

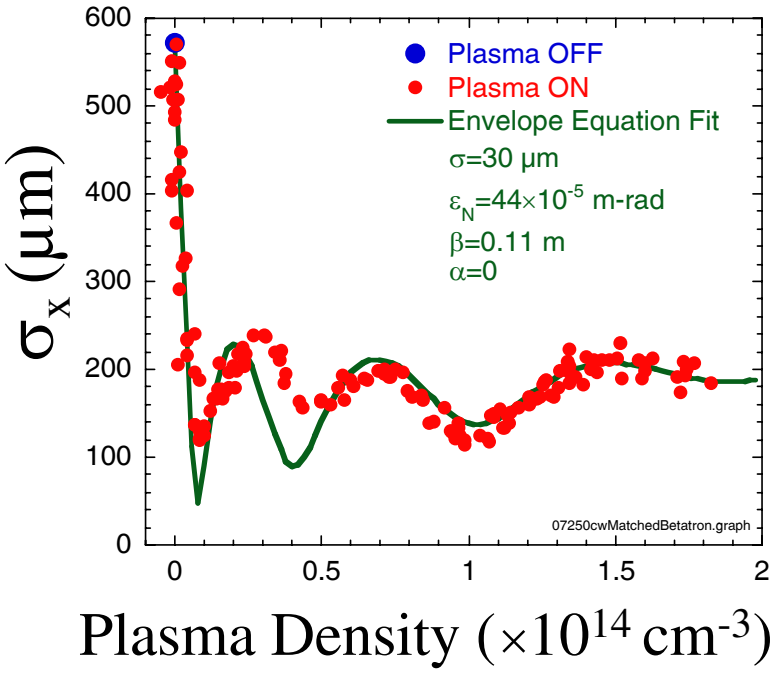

Figure A.7: Variation of the transverse spot size of the beam vs. plasma density. Initially the beam emittance force is larger than the plasma focusing force. As the two forces become equal the beam spot oscillations damp out and the bean is said to be "matched."

A breakthrough, which produced unambiquous results, was the conversion of the dispersion (dipole) magnet into a proper imaging spectrometer. This together with a streak camera to time resolve the dispersed images of the beam lead to clear evidence for energy loss of the bulk of the beam followed by energy gain of the latter slices of the beam.

Figure A.8 shows the change in energy of the picosecond wide slices of the beam. The peak energy loss and gain were about 160 MeV for a density of 1.8×10^{14} cm^{-3}. However, this number is for the centroid of the slice. The maximum energy gain was ~ 275 MeV in good agreement with 3D PIC code simulations of our experiment.

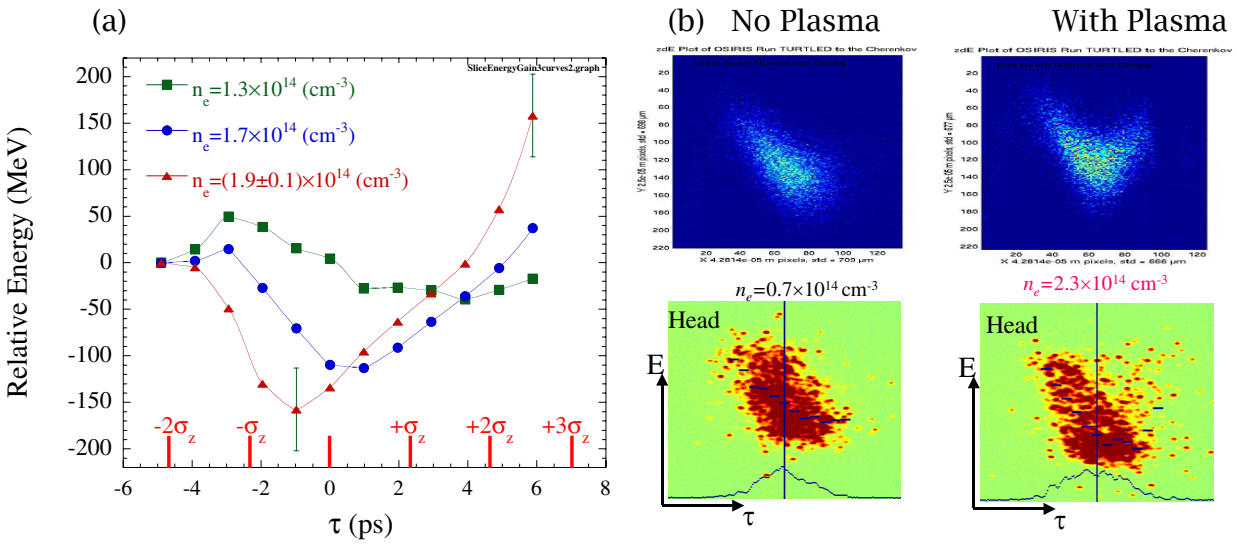

Figure A.8: (a) Relative change in energy of 1 ps wide slices of the beam at three different densities. At the highest density, energy loss of most of the beam slices and energy gain by the last two beam slices can clearly be seen. (b) PIC code simulations and corresponding streak camera data of energy dispersed slices of the beam without and with the plasma (E-162 experiment).

E-162

A.8 Halo Formation Around Positron Beam Core

P. Muggli et al., to be submitted for publication

The understanding of how intense, ultra-relativistic electron and positron beams propagate through meter-scale, dense plasmas critical to the development of a beam-driven, plasma wakefield accelerator. In particular, any physical effect that can degrade the transverse emittance of the beam as it traverses the plasma is deleterious to the final luminosity that can be achieved in this scheme. For instance, the extremely nonlinear transverse wakefields induced in the plasma by a positron beam can increase the slice emittance of the beam. This manifests itself by forming a halo around the core of the positron beam. Although much work has been done on understanding how beam halos are formed in space-charge dominated electron and ion beams, there is not work done on halo formation around an ultra-relativistic positron beam. In this case, it is the nonlinear focusing forces and not the space charge that is responsible for the loss of beam particles from the core to the halo.

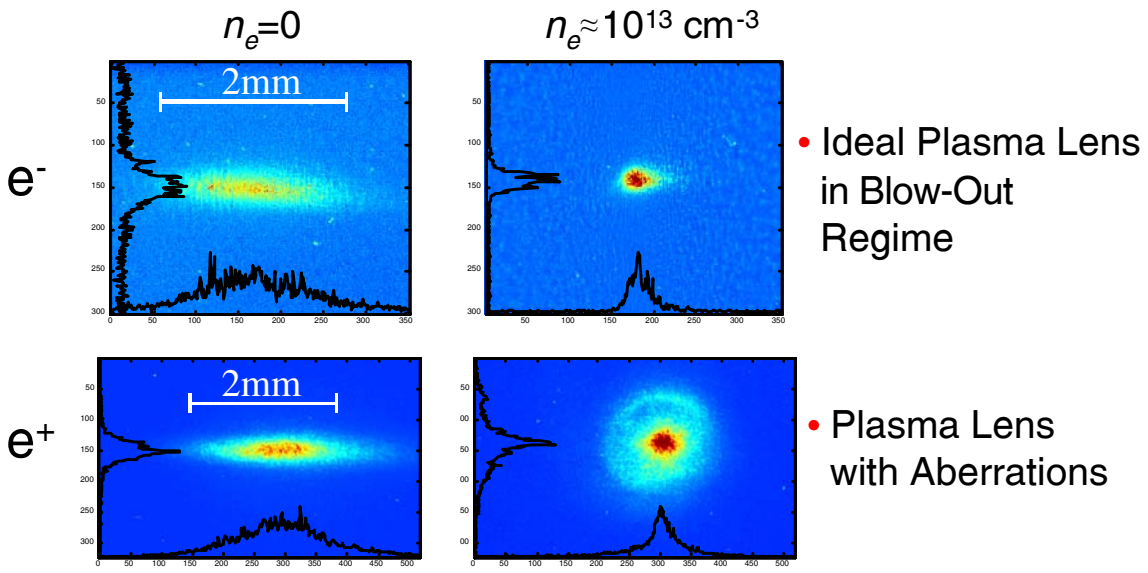

Figure A.9: The difference between focusing of grossly asymmetric ultra-relativisitic electron and positron beams by an underdense plasma lens. The electron beam shows a clear tightly focused spot while the positron beam displays a focused core surrounded by a halo indicative of an aberrated lens.

As part of E-162 we carried out the first experimental and numerical study of halo formation in a high charge (3 nC), ultra-relativistic (28.5 GeV) positron beam after propagating through a 1.4 m long, dense ($n_e \leq 5 \cdot 10^{14}$ cm^{-3}) plasma column. This is done by analyzing the images of the beam before and after the plasma. The beam entering the plasma has an emittance ratio ($\varepsilon_x/\varepsilon_y$) of 5. As the plasma density is increased, the core of the beam exiting the plasma is seen to be nearly symmetric with more and more particles contributing to the halo that surrounds this core. Simulations of the experiment using a particle-in-cell code give a good agreement on both the beam spot-size and the fraction of particles in the core with the experimental measurements. Simulations indicate that the slice emittance of the beam increases along the bunch and that an incoming beam with grossly unequal emittances, exits the plasma with approximately equal emittances in both transverse planes. This is clearly seen in Figure A.9. This self-matching of the beam to the plasma through emittance growth is a characteristic particular to positron beams.

A.9 Plasma Formation by field Induced Ionization by the Electron Beam

C. O'Connell et al., to be submitted for publication

The original idea of E-164 was to increase the average gradient of the PWFA from 100 MeV/m (seen in E-162) to 5 GeV/m by reducing the pulse length from 700μm to 100 μm. It was pointed out by Dr. Bruhwiler at the Advanced Accelerator Conference 2002 that as the beam became shorter the transverse electric field of the beam itself would eventually field-ionize the atoms and produce a plasma. Furthermore, the transverse size of the plasma can be larger than the beam.

In Run 1 of E-164, this field ionization became apparent for the first time. At a charge of $N = 1.2 \cdot 10^{10}$, σ_z = 100 μm and σ_r = 20 μm, the beam modified the plasma density via field-ionization (also called tunnel-ionization) at the peak of the beam (see Figure A.10). However, because we were at the threshold for field-ionization, the plasma formation was not very reproducible and in any case there were not too many beam particles left in the back of the beam to "see" the accelerating phase of the wake. It was decided therefore to go to even shorter bunches in E-164 Run II to increase the electric field associated with the beam.

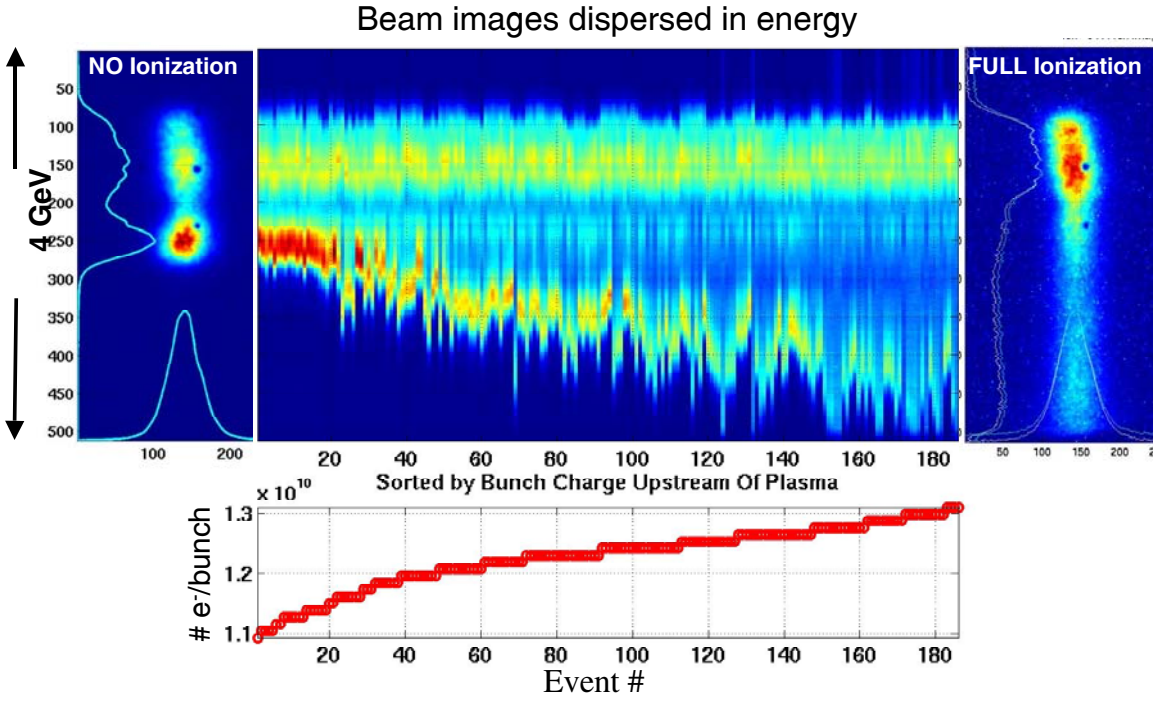

Figure A.10: The change in beam energy as a function of beam charge in the E-164 Run I. Up to 1.2 x 10^{10} electrons the beam energy spectrum shows only a slight change. For a charge greater than 1.2 x 10^{10} the electric field of the beam ionizes the Li and produces a fully ionized plasma. A wake response leads to the beam suddenly losing more than 1 GeV energy.

We have taken an extensive amount of data on field ionization of H_2, He, NO and Li by varying the beam charge, beam spot size, and the pulse width. The diagnostic of the onset of the plasma formation is the sudden onset of energy loss experienced by the main body of the beam whereas the diagnostic of formation of a fully ionized plasma is the eventual saturation of this energy loss at some maximum value.

E-164X

A.10 Observation of Greater Than 3 GeV Energy Gain

To be published

E-164X has demonstrated energy gain of more than 1 GeV in a 10 cm long plasma. This is both the largest energy gain ever achieved by a plasma accelerator and the largest accelerating gradient ever achieved by a beam driven plasma wakefield accelerator. The results were made possible by the combination of short electron bunches (~30 μm or 100 fs) and field ionized plasmas in the $3 \cdot 10^{17}$ cm^{-3} density range.

In previous experiments where the bunches were > 1ps the energy changes imparted by the plasma wakefield were of the same order or smaller than the incoming energy spread. To directly measure the effects of the plasma wakefield we used a streak camera to time resolve the energy spectrum and compare plasma on and off events (**Figure A.8**).

With the 100 fs bunches in E-164X it is no longer possible to time resolve the energy spectrum and the energy changes imparted by the plasma must be larger than the 1.2 GeV (full width) energy spread of the incoming bunch. Longitudinal wakefields in the main linac impose an additional challenge by giving the particles in the back of the bunch (which we accelerate) the lowest incoming energy. Thus, particles in the back of the bunch must be accelerated by more than 1.2 GeV before energy gain can be observed. **Figure A.11** shows the energy spectrum for two similar bunches with and without the 10 cm long $2.7 \cdot 10^{17}$ cm^{-3} plasma.

Typically about 7% of the incoming $2 \cdot 10^{10}$ electrons are accelerated to energies greater than the maximum incoming energy, with some particles gaining more than 3 GeV. We have observed many such events and the acceleration signal is consistent and reproducible.

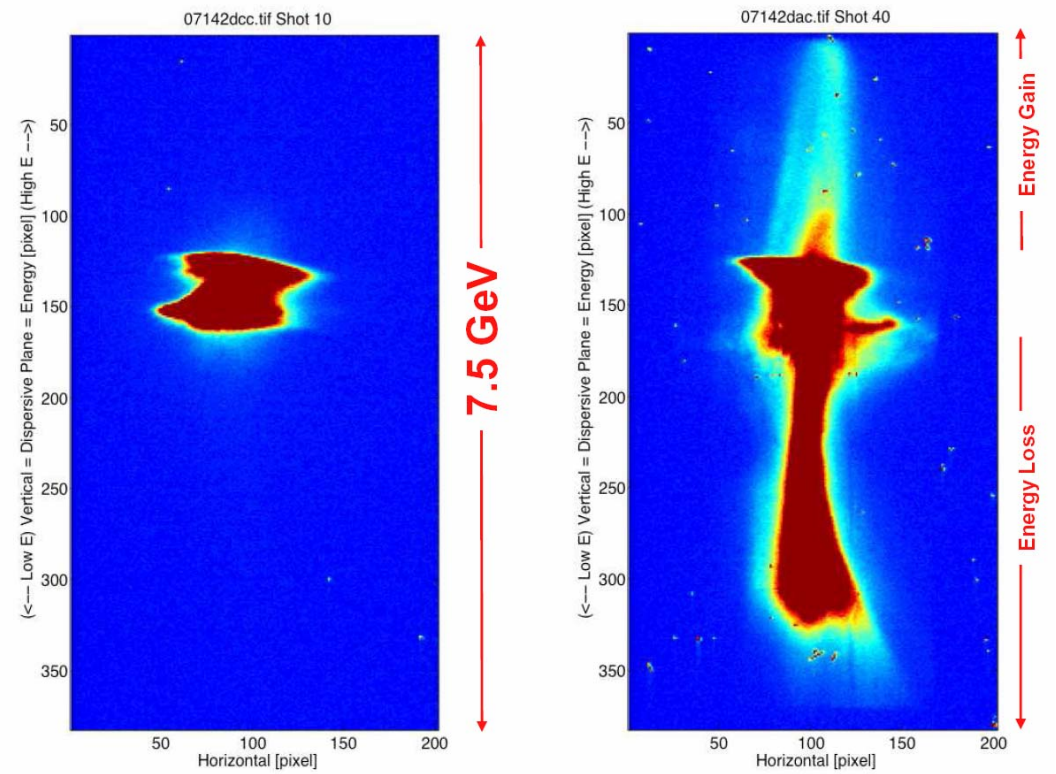

Figure A.11: The energy spectrum of the nominally 35μm long electron beam without the plasma and after it traverses the 10 cm long plasma. The beam has an approximately 1.5GeV head-to-tail energy spread. With the plasma on, one can clearly see energy loss of the bulk of the beam and energy gain of the tail particles in the beam.

B Publications

B.1 Peer-Reviewed Publications from E-157 / E-162 / E-164 / E-164X

1) M. J. Hogan *et al,* "E-157: A 1.4 Meter-Long Plasma Wakefield Acceleration Experiment Using A 30 GeV Electron Beam From The Stanford Linear Accelerator Center Linac", Physics of Plasmas **7**, 2241 (2000).

2) P. Muggli *et al,* "Collective Refraction Of A Beam Of Electrons At A Plasma-Gas Interface", Nature **411**, 43 (3 May 2001)

3) P. Catravas *et al,* "Measurements Of Radiation Near An Atomic Spectral Line From The Interaction Of A 30 GeV Electron Beam And A Long Plasma", Physical Review E **64** 046502 (2001).

4) P. Muggli *et al*, "Collective Refraction Of A Beam Of Electrons At A Plasma-Gas Interface", Physical Review Special Topics - Accelerators and Beams **4**, 091301 (2001).

5) S. Lee *et al*, "Energy Doubler For A Linear Collider", Physical Review Special Topics - Accelerators and Beams **5**, 011001 (2002).

6) Shouqin Wang *et al,* "X-Ray Emission From Betatron Motion In A Plasma Wiggler", Physical Review Letters **88**, 135004 (2002)

7) C. E. Clayton *et al,* "Transverse Envelope Dynamics Of A 28.5 GeV Electron Beam In A Long Plasma", Physical Review Letters **88**, 154801 (2002)

8) C. Joshi *et al,* "High Energy Density Plasma Science With An Ultra-Relativistic Electron Beam", Physics of Plasmas **9**, 1845 (2002).

9) C. O'Connell *et al*, "Dynamic Focusing Of An Electron Beam Through A Long Plasma", Physical Review Special Topics – Accelerators and Beams **5**, 1121301 (2002)

10) M. J. Hogan *et al*, "Ultrarelativistic-Positron-Beam Transport through Meter-Scale Plasmas", Physical Review Letters **90**, 205002 (2003).

11) B. Blue *et al*, "Plasma Wakefield Acceleration of an Intense Positron Beam", Physical Review Letters **90**, 214801 (2003).

12) C. Joshi and T. Katsouleas, "Plasma Accelerators at the Energy Frontier and on Tabletops", Physics Today, 47 (June 2003).

13) P. Muggli *et al*, "Meter-Scale Plasma-Wakefield Accelerator Driven by a Matched Electron Beam", Physical Review Letters **93**, 014802 (2004).

14) R. Maeda et al., "On the Possibility of a Multi-bunch Afterburner for Linear Colliders", Phys. Rev. ST Accel. Beams 7, 111301 (2004).

B.2 Related Peer-Reviewed Simulation Papers

1) S. Lee *et al,* "Simulations Of A Meter-Long Plasma Wakefield Accelerator", Physical Review E **61**, 7014 (2000)

2) R. G. Hemker *et al, "*Dynamic Effects In Plasma Wakefield Excitation", Physical Review Special Topics – Accelerators and Beams **3**, 061301 (2000).
3) S. Lee *et al*, "Plasma-Wakefield Acceleration Of A Positron Beam", Physical Review E **64**, 045501(R) (2001).
4) E. S. Dodd *et al*, "Hosing And Sloshing Of Short-Pulse GeV-Class Wakefield Drivers", Physical Review Letters **88**, 125001 (2002).
5) S. Deng et al, "Plasma wakefield acceleration in self-ionized gas or plasmas", Physical Review E **68**, 047401 (2003)

B.3 Papers in preparation – titles are tentative

1) P. Muggli et al., "Halo Formation Around Positron Beam Core"
2) C. O'Connell et al., "Plasma Formation by field Induced Ionization by the Electron Beam"
3) "Measurement Of Electron Acceleration In A Plasma Wakefield Accelerator" - intended for Science or Nature

B.4 Student Theses

1) Brent E. Blue, M.S. UCLA, "Hosing Instability of the Drive Electron Beam in the E-157 Plasma-Wakefield Acceleration Experiment at the Stanford Linear Accelerator" December 2000.
2) Seung Lee, Ph.D. USC, "Non-linear Plasma Wakefield Acceleration: Models and Experiments". May 2002.
3) Sho Wang, Ph.D. UCLA, "X-ray Synchrotron Radiation in a Plasma Wiggler" June 2002.
4) Brent E. Blue, Ph.D. UCLA, "Plasma Wakefield Acceleration of An Intense Positron Beam" January 2003
5) Wei Lu, M.S. UCLA, "Some Results on Linear and Nonlinear Plasma Wake Excitation : Theory and Simulation Verification"
6) Chenkun Huang, M.S. UCLA, "Development of a Novel PIC code for Studying Beam-Plasma Interactions"

B.5 Student Theses in Preparation

1) Caolionn O'Connell, Ph.D. Stanford, "Field Ionization of Neutral Lithium Vapor using a 28.5 GeV Electron Beam"
2) Devon Johnson, Ph.D. UCLA, "Positron production in a plasma wakefield accelerator"
3) Chris Barnes, Ph.D. Stanford, "Phase space determination in the FFTB and investigation of hosing effects"
4) Chengkun Huan, Ph.D. UCLA, "Quasi-static Particle-In-Cell modeling of Beam-Plasma Interactions"
5) Miaomiao Zhou, Ph.D. UCLA, "Accelerating ultra-short electron/positron bunches in field ionization produced plasmas"

6) Erdem Oz, Ph.D. USC, “Plasma Dark Current in Plasma Wake Field Accelerators (PWFA)”
7) Suzhi Deng, Ph. D. USC, “Models and Physics of Plasma Wakefield Accelerators in Beam-ionized gases”
8) Wei Lu, Ph. D. UCLA, “A theoretical formalism for wake excitation and acceleration in the blowout regime”

More than 15 invited presentations and/or papers at conferences, workshops, universities, and laboratories.

C References

1 C. Joshi and T. Katsouleas, Plasma Accelerators at the Energy Frontier and on Table-tops, Physics Today, 47 (June 2003)
2 M. Tigner, Accelerator R&D. Eur. Phys. J. C 33, s01, s146–s148 (2004), http://dx.doi.org/10.1140/epjcd/s2003-03-017-5
3 Y. B. Fainberg et al., Wakefield excitation in plasma by a train of relativistic electron bunches. Fizika Plazmy vol. 20, pp. 674-681, 1994.
4 S. Lee et al., Phys. Rev. ST Accel. Beams **5**, 011001 (2002)
5 C. O’Connell, “Field Ionization of Neutral Lithium Vapor using a 28.5 GeV Electron Beam”. PhD thesis, Stanford University, to be published.
6 J. Seeman, W. Brunk, R. Early, M. Ross, E. Tillmann and D. Walz, SLC Energy Spectrum Monitor using Synchrotron Radiation. 1986 Linear Accelerator Conference Proceedings, SLAC-PUB-3945, June 1986.
7 P. Emma, K. Bane, „ A Fast Longitudinal Phase Space Tracking Code with Graphical User Interface”, PAC 2005, to be published.
8 M. Borland, "elegant: A Flexible SDDS-Compliant Code for Accelerator Simulation,". Advanced Photon Source LS-287, September 2000.